DISSERTATIONES
CHIMICAE
UNIVERSITATIS
TARTUENSIS
167

RAIT KIVI

Allostery in cAMP dependent protein kinase catalytic subunit

DISSERTATIONES CHEMICAE UNIVERSITATIS TARTUENSIS
167

DISSERTATIONES CHEMICAE UNIVERSITATIS TARTUENSIS
167

RAIT KIVI

Allostery in cAMP dependent protein kinase catalytic subunit

UNIVERSITY OF TARTU
Press

Institute of Chemistry, Faculty of Science and Technology, University of Tartu, Estonia

Dissertation was accepted for the commencement of the degree of *Doctor philosophiae* in Chemistry at the University of Tartu on 15th of September 2017 by the Council of Institute of Chemistry, Faculty of Science and Technology, University of Tartu.

Supervisors: Prof. Jaak Järv
Institute of Chemistry, University of Tartu, Estonia

Prof. Mart Loog
Institute of Technology, University of Tartu, Estonia

Oponent: Dr. Varfolomeev S. D.
Director of N. Emanuel Institute of Biochemical Physics of RAS, Moscow, Russia

Commencement: 21st of November 2017 at 14:30, Ravila 14A-1020, Tartu

This work was funded by the Estonian Ministry of Education and Science (IUT14-20). Kristjan Jaak and DoRa T6 travel grants by Foundation Archimedes were granted to Rait Kivi to fund this work. This work has been partially supported by Graduate School of Functional materials and technologies receiving funding from the European Regional Development Fund in University of Tartu, Estonia.

ISSN 1406-0299
ISBN 978-9949-77-596-5 (print)
ISBN 978-9949-77-597-2 (pdf)

Copyright: Rait Kivi, 2017

University of Tartu Press
www.tyk.ee

TABLE OF CONTENTS

LIST OF ORIGINAL PUBLICATIONS

The following thesis is based on the following papers:

I. Kinetics of acrylodan-labelled cAMP-dependent protein kinase catalytic subunit denaturation. **Kivi** R, Loog M, Jemth P, Järv J. Protein J. 2013 Oct;32(7):519–25. Doi: 10.1007/s10930-013-9511-4.

II. Thermodynamic aspects of cAMP dependent protein kinase catalytic subunit allostery. **Kivi** R, Jemth P, Järv J. Protein J. 2014 Aug;33(4): 386–93. Doi: 10.1007/s10930-014-9570-1.

III. Computational modeling of acrylodan-labeled cAMP dependent protein kinase catalytic subunit unfolding. Kuznetsov A, **Kivi** R, Järv J. Comput Biol Chem. 2016 Apr;61:197–201. Doi: 10.1016/j.compbiolchem.2016.01.004.

IV. Different States of Acrylodan-Labeled 3'5'-Cyclic Adenosine Monophosphate Dependent Protein Kinase Catalytic Subunits in Denaturant Solutions. **Kivi** R, Järv J. Protein J. 2016 Oct;35(5):331–339.

V. Allosteric Effect of Adenosine Triphosphate on Peptide Recognition by 3'5'-Cyclic Adenosine Monophosphate Dependent Protein Kinase Catalytic Subunits. **Kivi** R, Solovjova K, Haljasorg T, Arukuusk P, Järv J. Protein J. 2016 Dec;35(6):459–466.

Author's contribution

I. The author planned and performed the experiments, participated in data processing and analysis and helped writing the manuscript.

II. The author planned and performed the experiments, participated in data processing and analysis and helped writing the manuscript.

III. The author participated in planning the experiments, participated in data analysis and interpretation and helped writing the manuscript.

IV. The author planned and performed the experiments, participated in data processing and analysis and helped writing the manuscript.

V. The author planned and participated in performing the experiments, participated in data processing and analysis and helped writing the manuscript.

ABBREVIATIONS

Acr	Acrylodan, 6-acryloyl-2-dimethylaminonaphthalene
AMP	Adenosine-5‘-monophosphate
AMPPNP	Adenosine-5‘-(β,γ-imido)triphosphate
ADP	Adenosine-5‘-diphosphate
ATP	Adenosine-5‘-triphosphate
ATPγC	β,γ-methyleneadenosine-5‘-triphosphate
BSA	Bovine serum albumin
cAMP	Cylclic adenosine-3‘,5‘-monophophate
DMSO	Dimethylsulphoxide
DTT	Dithiothreitol
EDTA	Ethylenediaminetetraacetic acid
HPLC	High performance liquid chromatography
IPTG	Isopropyl β-D-1-thiogalactopyranoside
MES	2-(N-morpholino)ethanesulfonic acid
MOPS	3-(N-morpholino)propanesulfonic acid
NMR	Nuclear magnetic resonance spectroscopy
PBS	Phosphate buffered saline
PKAc	cAMP-dependent protein kinase catalytic subunit from *M. musculus*
PKI[5–24]	A PKAc inhibitory peptide fragment from human protein kinase inhibitor protein TTYADFIASGRTGRRNAIHD
TRIS	Tris(hydroxymethyl)aminomethane

INTRODUCTION

Overall about one third of proteins translated in humans are phosphorylated at some point in their lifetime (Cohen, 2001). In cells phosphorylation is often utilized as mechanism for signal transduction, but it can also determine protein localization in different cell compartments, its activity and degradation timing. Addition of phosphoryl groups to proteins is made by enzymes called protein kinases, and one of the most widely studied member of this superfamily of enzymes is cAMP-dependent protein kinase (PKA) (Taylor et al., 2004). This kinase is present in all eukaryotic organisms studied so far, and it consists of two subunits: regulatory (PKAr) and catalytic (PKAc). As its catalytic subunit is a monomeric water-soluble protein in its active state, it has been a convenient tool to study regulatory phosphorylation mechanisms in general.

The regulatory phosphorylation reaction consists of transfer of the γ-phosphoryl group from ATP to the phosphorylatable protein or peptide. The phosphoryl group forms a covalent bond with a protein or peptide using its serine, threonine or tyrosine side chains. The phosphorylation reaction is catalyzed by protein kinases, which simultaneously bind both ATP and substrate protein or peptide, and this complex formation requires the presence of distinct binding sites on the surface of the kinase molecule. These binding sites are conventionally named as "nucleotide binding site", which is responsible for binding of ATP and its analogs, and "peptide binding site", responsible for interaction with the phosphorylatable of inhibitory peptide (Roskoski Jr., 2015).

Formation of the ternary complex, consisting of protein, ATP and the phosphorylatable peptide/protein allows direct transfer of ATP γ-phosphoryl to the acceptor hydroxyl group. Each substrate binding site has its characteristic selectivity and affinity (Taylor et al., 2004). Today it is also known that there can exist a kind of crosstalk between these binding sites as ligand binding to one of these sites can affect binding effectiveness of the other substrate. This phenomenon is called allosteric regulation or more simply allostery (Tsai and Nussinov, 2014).

Ligand binding effectiveness is determined by a network of weak non-covalent bonds between the ligand molecule and its binding site, formed in the process of complex formation and making up the enthalpy component of the binding free energy. The entropy component of this free energy change reflects changes of solvation and conformational freedom in the same process. These interactions and changes are well documented in the case of many kinases, and perhaps in the most detailed way in the case of PKAc (Masterson et al., 2010, 2011a).

The relatively simple structure of PKAc has allowed investigation of ligand binding with the free enzyme using fluorescence spectroscopy approach, where a fluorescent probe is covalently attached to the protein. As fluorescence of this probe is very sensitive to changes to its microenvironment, it can be used for monitoring processes, which change enzyme structure and concurrently the

positioning of this probe. Initially there were attempts to use this fluorescence probing to follow protein structural changes, which accompany ligand binding to PKAc. However, these changes of fluorescence were rather small, and no influence of peptide substrates binding on probe emission was observed (Lew et al., 1997a). Therefore, we modified this approach and studied ligand binding by measuring the stability of the enzyme, as denaturation of the protein was very clearly seen in the fluorescence spectrum of the label and rate of this process was sensitive to ligand binding. Interestingly, similar principles have been recently used in other denaturation assay methods, proposed for high-throughput screening of ligand binding effectiveness.

In this study, the acrylodan-labelled enzyme was prepared and used for analysis of protein denaturation mechanism, thermodynamic aspects of allostery in ligand binding, and the influence of peptide structure on allosteric phenomena.

LITERATURE OVERVIEW

1.1. Cyclic adenosine monophosphate dependent protein kinase

Protein kinases play a central role in various cellular functions (Manning et al., 2002). Together with phosphatases they form molecular switches which can control different aspects of protein functions, e.g. localization (Liku et al., 2005), activity (Ducommun et al., 1991) or degradation timing (Kõivomägi et al., 2011). Errors in protein regulation can have serious consequences for cells, which can express in different ways, for example through cell death or uncontrolled proliferation leading to formation of different tumors. This is the reason a lot of effort has been put into researching different signal transduction pathways and its components.

cAMP dependent protein kinase (PKA) is one of the 518 protein kinases in humans (Manning et al., 2002). So far, all sequenced eukaryotic organisms encode at least one copy of PKA in their genomes. PKA was discovered in 1968 by Walsh, Krebs and Perkins as a member in cAMP mediated signaling pathway (Walsh et al., 1968). In its inactive state PKA is a heterotetramer, consisting of 2 regulatory (PKAr) and 2 catalytic (PKAc) subunits (Corbin et al., 1978). Activation of PKA is mediated by an increase of cAMP concentration when 4 of these molecules bind to regulatory subunits. This will lead to the inactive tetramer dissociation and formation of 1 regulatory homodimer and 2 active catalytic monomers.

$$PKAr_2PKAc_2 + 4\ cAMP \rightarrow PKAr_2(cAMP)_4 + 2\ PKAc$$

PKA heterotetramers can bind to A kinase associated proteins (AKAPs) trough PKAr subunits. AKAPs act as a scaffold to facilitate optimum signal transduction by localizing PKA and other signaling enzymes with their substrates (Esseltine and Scott, 2013). There are 4 different PKAr and 3 different PKAc subunits in humans. As there is only one gene of PKAc, these isoforms arise through alternative splicing (Taylor et al., 2012a).

PKAc catalyzes the transfer of γ-phosphoryl group from ATP to a serine or threonine sidechain of a substrate protein.

1.2. Structure of PKAc

PKAc from *M. musculus* is a monomeric protein with molecular mass around 42 kDa. Crystal structure of PKAc was published in 1991 (Knighton et al., 1991a, 1991b), revealing, that it consist of small aminoterminal and large carboxyterminal lobes connected by a flexible hinge region. Catalytic cleft of PKAc is located between the lobes, where ATP binds to the ATP-binding

pocket. Small lobe is the main actor in ATP positioning: adenine ring forms hydrophobic interactions with small N-terminal lobe and flexible glycin-rich loop together with a lysin 72 sidechain positions ATP-phosphoryl tail in the correct position for phosphorylation reaction (Taylor et al., 2012b). A Mg^{2+} ion is also needed for the correct positioning of ATP phosphoryl tail. Protein substrate docking interface is on the large lobe.

Structure of PKAc is highly dynamic (Johnson et al., 2001). Crystallographic data have revealed 3 different conformations: 1) apo, where no ligands are bound to the protein, 2) secondary, where ATP is bound and 3) ternary, where both ATP and a peptide form a complex with PKAc (Taylor et al., 2004). In its apo form, where no ligands are bound to the protein, PKAc is in its „open" state, which means the small and large lobes are separated enough for the ATP or its analogues to bind to the ATP-binding pocket. After ATP binding to PKAc, the lobes approach each other and new inter- and intramolecular hydrophobic and polar interactions make the protein structure more compact and rigid. Protein substrate or inhibitor binding to the docking interface doesn't have as large stabilizing effect to the PKAc structure as ATP or its analogue inhibitors (Masterson et al., 2010).

1.3. Phosphorylation reaction

Enzymatic transfer of γ-phosphoryl group from ATP to a protein was discovered in 1954 when it was determined that a fraction of mitochondria from rat liver can phosphorylate casein (Burnett and Kennedy, 1954). Currently it is known that all kinases, exept pseudokinases, catalyze chemical reactions where a phosphoryl group from ATP is transferred to a substrate protein, where serine, threonine or tyrosine sidechain OH groups are phosphorylated:

$$MgATP^{1-} + \text{protein} - O{:}H \rightarrow \text{protein} - O{:}PO_3^{2-} + MgADP + H^+$$

For the catalysis reaction, both substrates need to be bound to the enzyme. In the case of PKAc, ATP is positioned in ATP-binding pocket so that the γ-phosphate protrudes to the surface in the way that lets it react with the protein substrate serine or threonine sidechain hydroxyl group (Knighton et al., 1991a).

1.4 Allosteric effects in binding and catalysis

Allostery can be described as a communication between ligand binding sites. Following this definition, binding of one ligand affects the binding of another ligand at a different binding site. This phenomenon is of fundamental importance in regulation and signaling events on a molecular level. Allostery can arise also through post-translational modification, most commonly through phosphorylation (Nussinov and Tsai, 2013).

The crosstalk between distinct ligand binding sites was first described in the case of binding of O_2 molecules to hemoglobin by Christian Bohr in 1903. The first plausible model for this phenomenon was given over 60 year later (Monod et al., 1965). A term "cooperative binding" was used in this context. Later, similar phenomena were observed with different ligands and that is reflected in term "allostery", pointing to structural differences of ligands. Finally, the presence of allosteric effects was recognized in single-subunit proteins, like PKAc.

There are several viewpoints how the phenomenon of allostery could be explained at the molecular level. The structural view of allostery tries to explain the modulation of substrate binding affinities by changes in protein structure, describing the exact networks of interactions between amino acids that form after ligand binding and affect binding properties of the other binding site (Tsai and Nussinov, 2014). This view agrees with the principles of "induced fit", stating that ligand binding alters protein structure and adjusts binding site properties by changing protein structure.

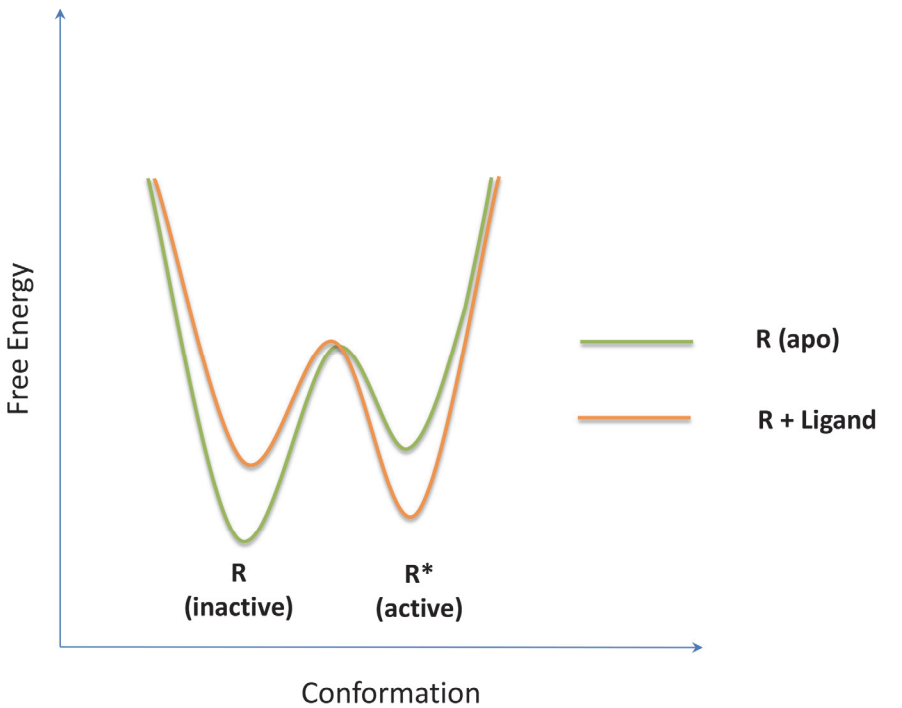

Figure 1. Example for thermodynamic view of allostery (Tsai and Nussinov, 2014). In this example there are two conformational populations present in the free-energy landscape of a protein: active (R*) and inactive (R). Free energy landscape in case of apo protein favors inactive population to be majorly populated (green line). When a ligand binds to the protein, free energy landscape is altered and active species population is energetically favorable (orange line) and therefore more populated.

Thermodynamic view of allostery postulates that allosteric effect arises through population shift towards protein states, which have better ligand binding properties, and these shifts are illustrated by change of the free energy landscape after the first ligand has bound to the enzyme. This conformational selection model is based on the fact that several structural protein isoforms, having different ligand binding properties, populate the free-energy landscape. Allosteric effect arises when the ratio between different populations shifts towards species, which bind the ligand with higher affinity.

1.5. Allosteric effects in PKAc

In this thesis, allosteric effect of PKAc is described in the context of binding of ligands that are involved in the phosphorylation reaction. Ligand binding and catalytic activity of PKAc can be taken together with the following scheme (1):

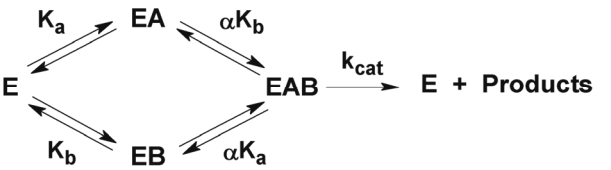

Scheme 1

where E is apo-PKAc, EA and EB are ligand bound PKAc, EAB is PKAc bound with both ligands, K_a and K_b are dissociation constants for ligands A and B respectively, α is an interaction factor. If $\alpha < 1$, then ligand binding is better in the case of pre-loaded complex and this means that we have positive allosteric effect. If $\alpha > 1$, then ligand binding with the complex is weaker and we have negative allostery. If $\alpha = 1$, then no allosteric modulation of binding effectiveness takes place.

Allosteric effects in PKAc reactions and ligand binding equilibria have been described by various groups over time. The first observation of PKAc ligand affinity modulation was noted in the study of the determination of kinetic mechanism of PKAc (Whitehouse and Walsh, 1983; Whitehouse et al., 1983), where the inhibition constant of inhibitor protein PKI varied depending on ATP presence up to 3 orders of magnitude. This result has later been tested and confirmed by other groups (Lew et al., 1997a). A more thorough view on PKAc allosteric properties was formulated in studies, where NMR spectroscopy was used for direct determination of binding effectiveness of ATP analog inhibitor and peptide with different protein ligand complexes (Masterson et al., 2008, 2011a, 2011b).

These results were in good agreement with earlier data, obtained by x-ray analysis of PKAc structure (Knighton et al., 1991a, 1991b; Taylor et al., 2004). These papers shed light on how ligands bind to PKAc and how different parts of PKAc interact with each other at different stages of ligand binding and

catalysis. The crystallographic and spectroscopic data have revealed, that PKAc has 3 main conformational states: apo or open state, where no ligands have bound to the protein; binary or intermediate state, where typically one ligand is bound to PKAc; and ternary or closed state, where both ligands are bound to the protein and which lobes are tightly pressed together. As these structual changes between different states are relatively large, it was proposed that allosteric communication between small and large lobes arise through hydrophobic networks (R and C spines) buried inside PKAc and that these intramolecular networks allosterically modulate ligand or inhibitor binding and subsequent catalysis (Kornev et al., 2008).

Using calorimetric methods, binding of phosphorylatable ligand and inhibitor were compared in terms of thermodynamics (Masterson et al., 2011a). In case of apo-PKAc, it revealed that for the peptide substrate PLN(1–20) (K_d=49 ± 8 μM) binding was entropy driven, as for the inhibitor peptide PKI[5–24] (K_d= 1.8 ± 0.4 μM), binding was enthalpy driven. It was also shown that binding of these peptides in the presence of ADP was enhanced by the factor of 5 and 40, respectively.

A detailed study of allosteric effects based of enzyme kinetics has been performed by Kuznetsov and Järv (Kuznetsov and Järv, 2008a). They quantified allosteric effect between ATP and different peptides and the principle „Better binding, stronger allostery“ was coined. This means that the better binders the ligands are, the stronger the allosteric effect between them becomes.

An interesting take on the allosteric cooperativity of PKAc was published recently, where inhibitor peptide PKI[5–24] binding to PKAc in presence of ATP analogues was studied using NMR (Kim et al., 2016). Modulation of PKI[5–24] affinity in presence of different ATP analogues is presented in Table 1. It was proposed that the allosteric effect depends on the openness of enzyme active site cleft. The more the lobes are in closed conformation, the larger the allosteric effect is. It was revealed, that the oxygen between β and γ phosphates of ATP plays a central role in allosteric network formation.

Table 1. PKI[5–24] affinities towards PKAc in presence of different ATP analogues.

Ligand	K_d (μM)	Cooperativity factor
Apo PKAc	6.4 ± 0.56	1
ATPγC	6.1 ± 0.27	1.0
AMP	5.7 ± 0.18	1.1
Adenine	1.5 ± 0.03	4.3
Adenosine	0.53 ± 0.02	12
ADP	0.23 ± 0.0097	29
AMPPNP	0.12 ± 0.0050	53
ATP	0.016 ± 0.0019	400

1.6 Acrylodan labelled proteins in ligand binding studies

Acrylodan (6-acryloyl-2- dimethylaminonaphthalene) is a fluorophore that is sensitive to its environmental properties (Prendergast et al., 1983). Namely, in polar solvents its fluorescence is quenched and emission maximum shifts towards longer wavelengths. In nonpolar environment, the fluorescence quantum yield improves and the emission maximum shifts toward shorter wavelengths. For example, if acrylodan is exited at 390 nm, the fluorescence emission maximum in 1,4-dioxane is at 435 nm, in acetonitrile at 468 nm, in ethanol at 502 nm, in methanol at 513 nm and in water at 540 nm. This property makes acrylodan a useful probe to study protein conformational changes, as the structural alterations are mirrored by change of fluorescence when the environment around the probe changes.

Acrylodan can have different emission spectra depending on the environment of the covalently bound dye in protein structure. For example, if acrylodan is bound to papain, its emission maximum is at 491 nm. In the case of troponin C, the emission maximum of acrylodan is at 510 nm, pointing to different microenvironment of the fluorescent dye in these proteins (Prendergast et al., 1983).

If a ligand binds to a protein, structural changes of its amino acid backbone and/or side chains can take place. If these structural movements, which change its surrounding environment, take place near acrylodan the fluorescence emission spectrum of the dye changes. For example, in titration of troponin C with Ca^{2+}, fluorescence emission maximum of this dye shifted from 510 nm to 517 nm (Prendergast et al., 1983).

Due to the micro-environment sensitivity, acrylodan has been used in different protein-binding assays as a versatile tool to probe structural changes in vitro. Recently it was used in a high-throughput assay of small molecules, which inhibit p38α (Simard et al., 2009). In this study, acrylodan was covalently bound to p38α activation loop, which controls its catalytic activity. This modified protein was then used to scan about 36000 small-molecule inhibitors to find specific inhibitors that bind to a catalytically inactive p38α species. Acrylodan has also been utilized as a sensor linked to a protein for detecting glutamic acid concentration (Wada et al., 2003).

1.7. Studies with acrylodan-labelled PKAc

Acrylodan-labelled PKAc was used to study ligand binding with the protein and to characterize mutual effect of peptides and nucleotide analogs on effectiveness of their binding (Lew et al., 1997a). The effects observed were named “synergistic ligand binding”. In this study, PKAc was modified in position 326 by change of asparagine to cysteine. This position is situated in the linker region near ATP-binding pocket, and the introduced cysteine was used to label PKAc with acrylodan. The mutated and labelled PKAc, further denoted as PKAc-acr,

was catalytically active and possessed similar ligand binding properties as the wild type protein. Fluorescence measurements revealed that, when excited at 395 nm, the emission maximum of the dye appeared at 498 nm. When titrated with different ligands that bind to the ATP-binding pocket, the emission maximum shifted towards longer wavelengths, and these shifts had maximal effect with ATP. At the same time the emission shift was accompanied with quenching of emission intensity. These findings indicated that binding of a ligand to the ATP-binding pocket induced structural changes and pushed acrylodan molecule partially out from its hydrophobic environment inside the protein interior. Therefore, this approach was used to describe nucleotide binding with the free enzyme and its complexes with nucleotides. Summary of these data is given in Table 2.

At the same time, if PKAc-acr was titrated with ligands targeting the peptide binding site on the protein surface, no changes in fluorescence were observed (Lew et al., 1997a). Consequently, peptides do not cause structural changes that would affect the local environment around acrylodan molecule. Therefore, effect of peptides on the enzyme conformation and allostery was not studied by these authors more thoroughly, and these investigations were one of the objectives of this dissertation, as the introduced method has universal applicability to study protein-ligand interactions.

Table 2. Dissociation constants of ATP-site targeted ligands in absence or presence of peptide inhibitors (μM). Data from (Lew et al., 1997a).

	PKAc-acr	**PKAc-acr + PKI[14–22]**	**PKAc-acr + PKI[5–24]**	**PKAc-acr + PKI**
ATP	25 ± 1.3	3.9 ± 0.7	0.0073 ± 0.0014	0.013 ± 0.0026
AMPPNP	182 ± 15	40 ± 7	3.4 ± 0.3	5.4 ± 0.6
ADP	24 ± 1.3	1.3 ± 0.4	Not determined	1.2 ± 0.14

Significant synergistic effects can be seen in Table 2, where ATP binding is enhanced in the presence of PKI by 19,000 times. For other combinations, the synergistic effects are smaller. These results were later analyzed and discussed as allosteric effects by Kuznetsov et al (Kuznetsov and Järv, 2008a, 2008b).

PKAc-acr has also been used in stopped-flow experiments to study catalytic mechanism of PKAc (Lew et al., 1997b).

1.8. Denaturation assays for protein-ligand binding study

Protein-ligand complex dissociation constants, which are commonly used for quantitative characterization of these complexes, can be calculated from the complex concentration versus ligand concentration plots, or by using similar dependences for some other parameters, which are proportional to the complex concentration and can be detected experimentally. For example, these calculations

can be made, using NMR data by measuring chemical shifts of certain protein or ligand atoms in the absence and presence of different ligands (Li and Kang, 2017). In case of isothermal titration calorimetry (ITC), ligand binding can be characterized by measuring heat that is released in the binding event. Surface plasmon resonance (SPR) can be used to detect binding to ligands that are attached to a surface. Various spectroscopic methods have been developed to determine ligand binding by detecting changes in protein structure that affect some fluorescent property of the ligand-protein complex (Fang, 2012). In case of enzymes, protein-ligand complexes can also be characterized by using kinetic data from equilibrium or pre-equlibrium stages of reaction.

In recent years, however, denaturation assay has become more popular as this methodology can be implemented for different analytical purposes. This approach is based on the fact that ligand binding stabilizes protein structure and slows down its denaturation, induced in the presence of some denaturing agent or by increase of temperature. This means that a protein, when bound to a ligand, has higher melting temperature or that it loses its structure at higher denaturant concentrations. In both of these cases it is assumed that the folding-unfolding transition is reversible (Senisterra et al., 2011; Vedadi et al., 2006).

Protein denaturation is usually detected by change of intrinsic (Mahendrarajah et al., 2011) or extrinsic fluorescence. Intrinsic fluorescence is emitted by amino acid residues encoded into protein structure. Extrinsic fluorescence can be emitted by fluorescent dye bound covalently to a protein or a free probe present in the reaction solution (de Araujo et al., 2017). These probes are sensitive to changes to their microenvironment and when a protein is denatured, the dyes penetrate towards now accessible hydrophobic cores which in turn change the emitted fluorescence that can be detected.

An important aspect of these methods is their universal nature, as there are no requirements about specific ligand properties, i.e. the presence of radioactive label, chromophores or fluorophores etc.

In this study, the kinetic version of the thermal ligand binding assay was developed. Following this procedure, kinetics of protein denaturation is measured in the absence and presence of different ligands and the ratio of denaturation rates versus ligand concentration plots are used for calculation of the ligand-protein dissociation constants.

OBJECTIVES OF DISSERTATION

The main objectives of this dissertation were:

1. Finding experimental method for monitoring interaction of ligands with the free PKAc, and application of this method for quantitative characterization of ligand binding equilibria.

2. Preparation of acrylodan-labelled PKAc and application of this adduct for ligand-protein interaction assay by studying kinetics of protein denaturation.

3. Investigation into mechanism of PKAc denaturation by chemical denaturants and computational modelling of this process.

4. Examination of influence of ligand structure on allosteric effect of ATP on peptide binding with PKAc.

5. Characterization of thermodynamic aspects of allosteric interactions in nucleotide and peptide binding with PKAc.

METHODS

3.1. Chemicals

Chemicals were obtained from Sigma-Aldrich, USA (ATP, BSA, H_3PO_4, TRIS-HCl, NaCl, $MgCl_2$, GndHCl, urea) and from Applichem, Germany (MES, MOPS). Peptides LRRASLG, RRYSV and PKI[5–24] were purchased from Biochem Ltd., China. Other peptides used for the study were synthesized using Fmoc solid-phase peptide synthesis strategy in Tartu. Acrylodan was from Anaspec, USA. γ–^{32}P was purchased from Amersham, UK. Phosphocellulose paper P81 and ion-exchange medium P11 were from Whatman, UK. All other chemicals used for the study were of the highest grade available. Buffers were made using Milli-Q water and filtered with 40μm filter. PCR and mutagenesis primers were from Microsynth, Switzerland.

3.2. Expression and purification PKAc and N326C PKAc

Detailed description of PKAc expression plasmid construction, protein expression and purification procedures can be found in our paper (Kivi et al., 2013). Shortly, using PCR, PKAc DNA sequence from *M. musculus* (Ensemble ID ENSMUST00000005606) was cloned from pET15b (SS Taylor, Add Gene, USA) into pET28a expression plasmid. Mutation N326C, necessary for protein labelling, was introduced by site-directed mutagenesis via ssDNA method. PKAc wild type (WT) and PKAc N326 C plasmids were transformed into *E. coli* Bl21DE. Protein expression was induced with 0.5 mM IPTG in 1 litre of 2xYT OD=0.6 at 18 °C for overnight on shaker. Cells were harvested by centrifugation for 5 minutes at 6000g at 4 °C. PKAc was purified using ion-exchange chromatography. Cells were lysed using French press at 15000 psi and centrifuged at 4 °C 43000g for 10 min. Phosphocellulose P11 from Whatman was added and left stirring overnight and subsequently packed into 1x15 column. Protein was eluted in 30 mM MES pH 6.5, 1 mM EDTA, 5 mM β–mercaptoethanol with 0–0.5 M KPO_4 linear gradient on Äkta Purifier system. PKAc WT fractions with significant A280 absorbance were checked with SDS-PAGE and fractions with protein bands sized about 45 kDA were selected and pooled for dialysis against 20 mM TRIS pH 7.5, 50 mM NaCl, 0.5 mM DTT, 1 mM EDTA, 20% glycerol. N326C mutant was also pooled and dialyzed as with PKAc WT or labelled with acrylodan. Purified protein was aliquoted and stored at –80 °C.

3.3. PKAc N326C labelling with acrylodan

PKAc N326C buffer was exchanged to 50 mM MOPS pH 8.0, 50 mM NaCl using PD10 column (GE Healthcare) gel chromatography. 1 mM ATP and 10 mM $MgCl_2$ was added and mixture was incubated for 1 h at 4 °C. Acrylodan was added to the reaction mixture with 5:1 molar excess compared to PKAc N326C and mixture was incubated overnight at 4 °C in the dark. Free label was removed using PD-10 columns equilibrated with 50 mM MOPS pH 7.0, 50 mM NaCl, 10% glycerol. Success of labelling reaction was assessed with SDS-PAGE under UV light and MS analysis (Thermo LTQ-Orbitrap).

3.4. Comparison of PKAc WT, PKAc N324C and PKAc-Acr activity in kemptide phosphorylation reaction

Kemptide (peptide LRRASLG) phosphorylation assay by PKAc was performed at 30 °C in 50 mM TRIS pH 7.5, 10 mM $MgCl_2$, 0.2 mg/ml BSA, 1000 μM ATP (with γ–^{32}P), peptide concentrations varied from 5 to 1000 μM. Reaction was started with the addition of PKAc. To assess initial rate of phosphorylation, 10 μL aliquots of reaction mixture were taken on to phosphocellulose paper discs and immersed in cold 25 mM H_3PO_4 at 5 different time points. The paper discs were washed 4 times in 25 mM H_3PO_4 and dried at 56 °C for 30 minutes. Radiation from aliquots was quantified using PhosphorImager Typhoon Trio system and ImageQuant software (GE Healthcare, USA). Values for initial Kemptide phosphorylation rate by PKAc was calculated from the slopes of the product concentration versus time plots.

3.5. Spectrofluorimetric measurements

Fluorescence measurements were performed either with a SLM 4800 Spectro-fluorimeter (SLM Instruments) or Horiba Scientific Fluoromax-4 spectrophoto-meter in 600 to 1200 μL quartz cuvettes. Fluorescence excitation wavelength was set to 395 nm, emission was monitored from 420 to 600 nm. Before data processing, a weak Raman band at 365 nm was subtracted from fluorescence emission data. Reaction mixture for denaturation assay consist of 50 mM MOPS pH 7.0, 10 mM $MgCl_2$, 50 mM NaCl, substrate and 50 nM PKAc-ACR. Measurements were started by the addition of PKAc to the reaction mixture and monitored as long as the protein denaturation process took place.

3.6 Analysis of fluorescence spectra

The experimental spectra were quantitatively analyzed by using a log-normal function proposed by Siano and Metzler (Siano and Metzler, 1969), and used for analysis of fluorescence of acrylodan adducts with the model peptide

Lys-Cys-Phe and some proteins (Emel'ianenko et al., 2000). Details of this procedure are described in (Kivi and Järv, 2016).

The calculations were based a log-normal function:

$$f(\nu) = f_{max} \exp\left[-\frac{ln2}{\ln^2(\rho)}\ ln^2\left(\frac{\alpha-\nu}{\alpha-\nu_{max}}\right)\right], \quad if\ \nu < \alpha$$
$$f(\nu) = 0, \quad if\ \nu \geq \alpha \qquad \text{Eq. 1}$$

where $f(\nu)$ is the emission intensity at wave number ν, f_{max} is the maximum intensity at the emission peak at ν_{max}, ρ and α are empirical parameters characterizing asymmetry of the band shape (skewness), depending on the positions of the two half-maximal intensity limits at ν_+ and ν_- values on both sides of the ν_{max} value. So, $\rho = (\nu_{max} - \nu_-)/(\nu_+ - \nu_{max})$ and $\alpha = \nu_{max} + \frac{\rho(\nu_+ - \nu_-)}{\rho^2 - 1}$. The physical meaning of the parameters α and ρ was discussed thoroughly in literature (Bacalum et al., 2013; Emel'ianenko et al., 2000), and in this study these variables were parameterized for acrylodan bound to distinct states of the acrylodan-labelled PKAc, and used as constraints for resolving emission spectra into overlapping bands.

This analysis was done by assuming that the overall fluorescence intensity at any ν value consists additively of contribution of each distinct emitting state, characterized by different f_{max} and ν_{max} values. Therefore the combination of the log-normal function (1) was used for estimation of the f_{max} values for each emitting state of the protein, using the separately determined ν_{max}, α and ρ values. Assuming that the amplitude of the fluorescence band was proportional to the concentration of the emitting state, and considering different emission yields, kinetic and equilibrium parameters of the system were calculated from these spectral data.

3.7. Data processing

Data processing was performed with Microsoft Excel for Mac (version 14.0.0) and GraphPad Prism 5.0 (GraphPad Software Inc., USA) software packages. Standard errors for fitted curve parameters were listed.

RESULTS AND DISCUSSION

4.1. Acrylodan labelled PKAc

To assess ligand binding to PKAc in the absence of catalytic reaction, we decided to use an acrylodan-labelled protein, where the fluorescence of the dye is sensitive to its microenvironment (Lew et al., 1997a). This approach was first used to study PKAc interaction with nucleotide ligands, while titration of the labelled enzyme with peptide ligands caused no change in the fluorescence spectrum (Lew et al., 1997a). Therefore, peptide binding studies were not made by using this method. The same conclusion was drawn on the basis of our preliminary studies.

To overcome this shortcut, a new method for assaying ligand binding to PKAc, was proposed in this work, based on denaturation kinetic measurements of protein in the absence and presence of ligands. Shortly, alteration of protein conformation was assayed by monitoring the reporter ligand fluorescence spectrum, which changed due to its movement from polar to apolar environment in the protein denaturation process. This approach was found to be an universal method for ligand binding assay in the case of PKAc, which may have implications for development of kinetic version of high throughput screening of drugs targeted at protein kinase active center.

4.1.1 Effect of mutation N326C and acrylodan labelling on PKAc catalytic properties

For preparation of the acrylodan-PKAc adduct, N326C mutant was expressed in *E. coli* and purified using ion-exchange chromatography. It was shown that catalytic and substrate binding properties of this protein as well as its acrylodan-labelled derivative were similar to the wild type enzyme. It was also demonstrated that mutation N326C allowed specific labelling of this protein with acrylodan (Figure 2), as only 4% of the label was bound at the native cysteine 199 and no unspecific labelling was detected at position 343. These results were in agreement with the data published before (Lew et al., 1997a).

Structure of the labelled PKAc was computationally simulated and the results of this analysis are shown in Figure 2. It can be seen that the dye molecule is located on the surface of the protein molecule that explains sensitivity of its fluorescence on conformational status of the protein.

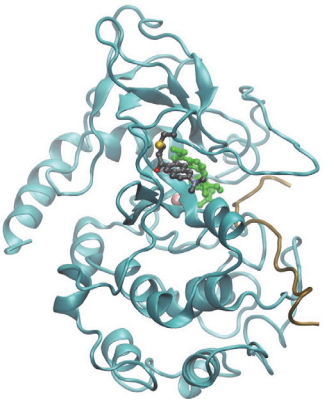

Figure 2. Illustration of PKAc labelled with acrylodan (black). ATP is colored green, peptide inhibitor PKI[5–24] colored brown. As can be seen from the computer simulation, acrylodan is bound to the surface of PKAc near the ATP-binding pocket.

To assess whether the introduced mutation N326C or its labelling with arcylodan affected catalytic properties of PKAc, we studied kinetics of phosphorylation of specific peptide substrate Kemptide (sequence LRRASLG) by the wild type enzyme, its mutant N326C and by the acrylodan-PKAc adduct. This study was done using conventional kinetic analysis and data were processed by the Michaelis-Menten rate equation $v=V_{max}*[S]/(K_m+[S])$, where [S] is kemptide concentration and Michaelis constant K_m and maximum velocity V_{max} are obtained from the plotted data (Figure 3).

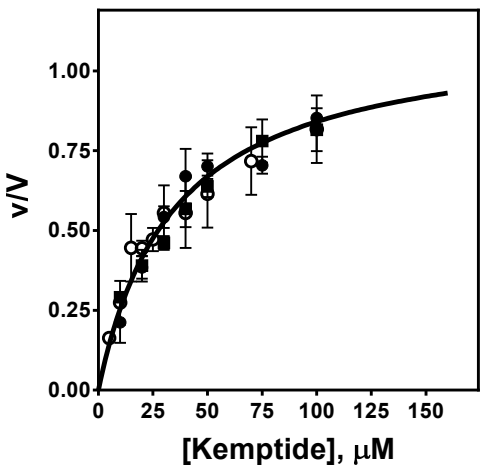

Figure 3. Kinetics of kemptide phosphorylation by wild-type PKAc (○), PKAc N326C (●) and PKAc N326C labelled with acrylodan (■). v/V marks relative reaction rate when compared to V_{max}. The similarity of kinetic parameters suggested that the mutation as well as acrylodan labelling did not alter the catalytic properties of the enzyme.

As seen from Table 3, PKAc wildtype, N326C mutant and N326C mutant labelled with acrylodan had similar K_m in all cases, leading to the conclusion that the mutation and subsequent labelling of PKAc did not change catalytic properties of the enzyme.

Table 3. K_m of Kemptide for different PKAc constructs.

PKAc	K_m, μM
Wildtype	27 ± 6
N326C	29 ± 5
N326C-acrylodan	26 ± 6

4.1.2 Fluorescence properties of acrylodan-PKAc adduct

When PKAc-acr was excited at 395 nm, emission spectrum with λ_{max}= 496 nm was observed (Figure 4A). This emission spectrum was significantly shifted when compared with λ_{max}= 540 nm of the acrylodan-thiol adduct in water. On the other hand, in 1,4-dioxane (and other organic solvents) the λ_{max} value of the emission spectrum of the acrylodan-thiol adduct was 435 nm (Prendergast et al., 1983). Therefore, it was suggested that in the case of acrylodan-labelled PKAc, the fluorophore molecule is positioned on the surface of the protein, and is partially shielded from interaction with water molecules. This suggestion agreed with our results of computational modeling of acrylodan-PKAc adduct structure, shown in Figure 2.

Structure of the cAMP-dependent protein kinase catalytic subunit, where asparagine residue 326 was replaced with acrylodan-cysteine conjugate to implement this fluorescence reporter group into the enzyme, was modeled using molecular dynamics (MD) method and the positioning of the dye molecule in protein structure was characterized at temperatures 300 K, 500 K and 700 K. It was found that the acrylodan moiety, which fluorescence is very sensitive to solvating properties of its microenvironment, was located on the surface of the native protein at 300 K that enabled its partial solvation with water. At high temperature, the protein structure significantly changed, as the secondary and tertiary structure elements were unfolded and these changes were sensitively reflected in positioning of the dye molecule. At 700 K complete unfolding of the protein occurred and the reporter group was entirely expelled into water. However, at 500 K an intermediate of the protein unfolding process was formed, where the fluorescence reporter group was directed towards the protein interior and buried in the core of the formed molten globule state. This different positioning of the reporter group was in agreement with the two different shifts of emission spectrum of the covalently bound acrylodan, observed in the unfolding process of the protein.

Interestingly, if acrylodan-PKAc adduct was heated at 100 °C for 5min, its fluorescence spectrum shifted towards shorter wavelengths (λ_{max}= 467 nm) and its intensity increased (Figure 4A). This change indicated that the dye molecule was shifted into less polar medium that is similar to organic solvents. Therefore, it was suggested that short thermal treatment of PKAc altered its structure and allowed acrylodan to penetrate inside the protein interior, where it is protected

from water. The computational modeling of denaturation process was in agreement with the in vitro experiments.

When acrylodan-PKAc complex was titrated with ATP or its analogues, red-shift in fluorescence spectrum was detected, as has been described before (Lew et al., 1997a). This red-shift of emission spectrum points to alteration of acrylodan microenvironment that accompanied ligand binding and subsequent changes in protein structure. It could be argued that these conformational changes partially expelled the dye molecule from the more hydrophobic environment around the ATP-binding pocket. In the case of peptide substrates, no change in fluorescence was detected under the same experimental conditions.

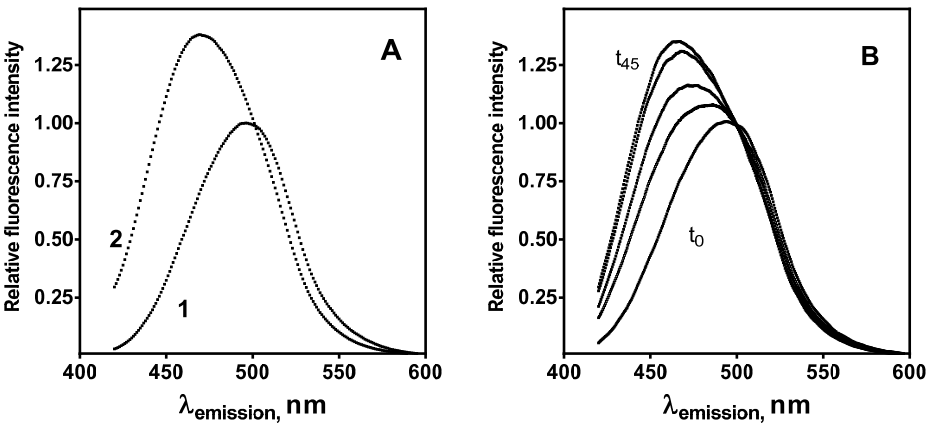

Figure 4. Influence of thermal denaturation in 50 mM TRIS-HCl (panel A) and chemical denaturation in 20 mM MOPS buffer (panel B) on fluorescence spectra of acrylodan-labelled PKAc. Spectra shown in panel A (left) were recorded at 25 °C before (1) and after temperature treatment (2) of the protein sample as described in text. Spectra shown in panel B were recorded in MOPS buffer at 25 °C at the following time points (starting from the lowest curve): 1, 5, 11, 21, 36, 45 min.

4.1.3. Denaturation kinetics of PKAc-acr adduct

We noticed that when PKAc-acr was incubated in MOPS buffer at around room temperature, the fluorescence of the protein changed over time (Figure 4B). Namely, its λ_{max} shifted from 496 nm to 467 nm, which was also accompanied by increase of fluorescence intensity, and this change was reproducible. By combining this phenomenon with the prior observation that thermal denaturation shifted λ_{max} to 467 nm, it was concluded that denaturation of PKAc takes place in 20 mM MOPS buffer. Additionally, when different ligands of PKAc were added to the reaction mixture, the rate of fluorescence change decreased (Figure 5) when compared to apo-PKAc denaturation.

When fluorescence values, monitored at different wavelengths, were integrated and plotted against time, it was possible to describe the process by the following rate equation:

$$F_t = F_0 + \Delta F_{max}\,(1 - e^{-k_{obs}t}) \qquad \text{Eq. 2}$$

where F_t is integrated fluorescence value at time t, F_0 is fluorescence value at t_0, ΔF_{max} is maximum fluorescence change amplitude, k_{obs} is observed reaction rate, t is time.

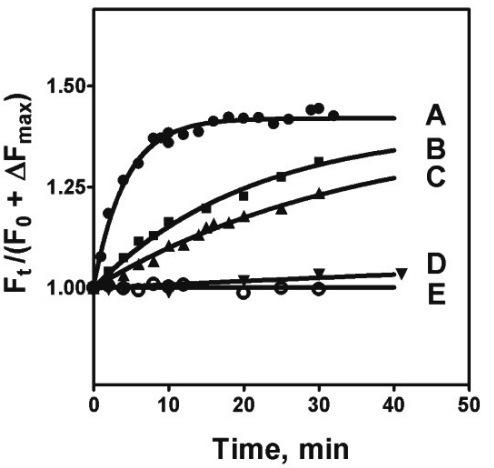

Figure 5. Time-course of fluorescence increase of 50 nM acrylodan labelled PKAc in 20 mM MOPS buffer at pH=7.0 and 25 °C (●, fitted curve **A**), and in the presence of 250 μM (▲, fitted curve **C**) or 2.5 mM (▼, fitted curve **D**) of ATP, or 1 μM (■, fitted curve **B**) of peptide inhibitor PKI[5–24], or the mixture of 250 μM ATP and 1 μM PKI[5–24] (○, fitted curve **E**).

When PKAc is in the reaction mixture without any ligands, protein denaturation can be presented by the following reaction scheme:

$$\mathrm{N} \xrightarrow{k_d} \mathrm{D} \qquad \text{Eq. 3}$$

where N denotes active enzyme, D is denatured protein and k_d is denaturation rate constant. If there are ligands present in the assay mixture, the overall denaturation rate depends on ligand concentration and its affinity, and this influence can be summarized by the following reaction scheme:

$$\mathrm{NL} \overset{K_L}{\rightleftharpoons} \mathrm{N} \xrightarrow{k_d} \mathrm{D} \qquad \text{Eq. 4}$$

where N is active enzyme, D is denatured enzyme, NL is enzyme-ligand complex, K_L is ligand dissociation constant, k_d is denaturation rate constant. If the equilibrium between NL and N is reached relatively fast when compared to denaturation process, the overall apparent denaturation rate should follow the first-order rate equation (Eq. 2), and the apparent rate constant k_{obs} should depend on ligand concentration and its affinity K_L (Eq. 5):

$$k_{\mathrm{obs}} = \frac{k_{\mathrm{d}}}{1 + \frac{[L]}{K_L}} \qquad \text{Eq. 5}$$

It can be seen that the dependence of k_{obs} vs ligand concentration allows calculation of the K_L value, and this can be done by using the linear transformation of the rate equation (Eq. 5) in coordinates of k_d/k_{obs} and $1+[L]/K_L$. To test the validity of the assumptions made about PKAc denaturation, we measured its denaturation rates in presence of ligands with known dissociation constants (Figure 6). As can be seen from this figure, there was a good agreement between literature data and our results.

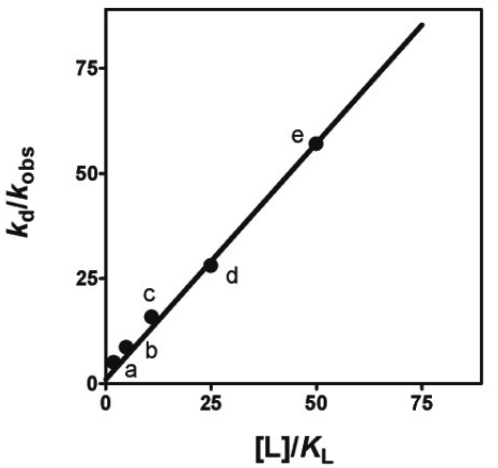

Figure 6. The dose-dependent stabilization of the acrylodan-labelled PKAc by: 1 μM PKI[5–24] (a) with K_L= 0.4 μM (Zheng et al., 1993); 250 μM (b) and 2.5 mM (e) ATP with K_L= 48 μM (Lew et al., 1997a); 20 μM (c) and 50 μM (d) peptide substrate RRYSV with K_L= 2.0 μM (Kuznetsov and Järv, 2008b). Experiments were made in 20 mM MOPS buffer at pH 7.0 and 25 °C, except data for RRYSV which were obtained at 30 °C.

These results confirm that the proposed kinetic version of the denaturation assay of binding properties can be used to determine ligand dissociation constants in this system, and more importantly, binding effectiveness of both nucleotide and peptide analogs can be determined.

4.2. Mechanism of PKAc-acr adduct denaturation

To strengthen the conclusion stated above and to extend our understanding of the processes which causes alteration of fluorescence spectra of acrylodan-PKAc adduct, a series of experiments were made with urea and guanidine hydrochloride, which are classical denaturing agents. These experiments were performed in Tris buffer (50 mM TRIS pH 7.4, 10 mM $MgCl_2$, 50 mM NaCl), where the protein was stable and no spectral shifts of fluorescence were observed during several hours. This state was denoted as native enzyme and marked by N in reaction Eq. 3 and 4.

At moderate denaturant concentrations, which were up to 1 M for guanidine hydrochloride and up to 2.5 M urea, fluorescence maximum of the dye shifted to 467 nm, and this shift was accompanied by increase in fluorescence intensity. The same result was observed in MOPS buffer, where the fluorescence maximum shifted to shorter wavelengths and increase in fluorescence intensity was observed. This change of fluorescence suggested that the fluorophore moved into more hydrophobic environment, possibly penetrating towards the protein hydrophobic core. As above, this state was denoted as denatured enzyme and labelled by D in Eq. 3 and 4.

If urea or guanidine hydrochloride concentration was increased, fluorescence of the acrylodan-PKAc adduct shifted towards longer wavelengths with maximum at 516 nm at the higher denaturant concentrations. This shift was accompanied by decrease of fluorescence intensity. These changes indicate that the acrylodan residue was moved into a more hydrophilic environment, if compared with native or denatured states. These changes could be explained by loss of protein structure at high denaturant concentrations and exposure of the dye molecule to water environment. Therefore, this state was denoted as unfolded protein and marked by U in reaction schemes.

Proceeding from the understanding that the acrylodan-PKAc adduct can have three distinct states, the fluorescence spectra were decomposed into three components and this analysis allowed quantification of these three protein states, N, D and U, respectively. Using this method, the fluorescence spectra were decomposed into these three constituent parts, and dependence of population of these states at different denaturant concentrations was obtained, as shown in Figure 7.

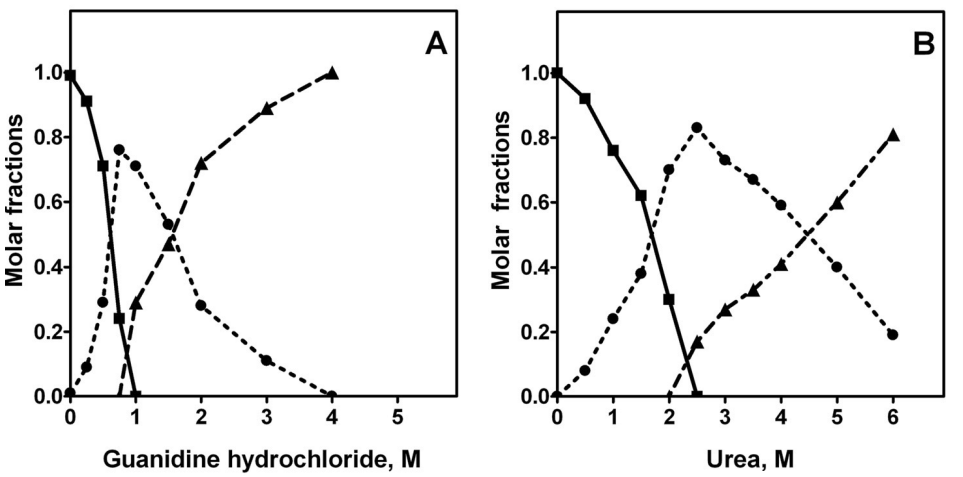

Figure 7. Fractional distribution of acrylodan-labelled PKAc conformations at different concentrations of guanidine hydrochloride (left) and urea (right). Fractions of natural (active) state (■), denatured state (●) and unfolded state (▲) were shown.

Interestingly, the process observed in 20 mM MOPS solution ended with formation of the state D. Therefore, this buffer can be regarded as a chemical denaturant, which acts at rather low concentration, and leads to formation of the protein state D at the used concentration, while for unfolding of the protein probably much higher MOPS concentrations are needed. This means that application of MOPS buffer was a good choice for our kinetic denaturation assay, as experiments could be made at different temperatures, including the interval of low temperatures, and at rather low denaturant concentrations.

All the above-mentioned conclusions about structural changes of acrylodan-PKAc adduct during the denaturation and unfolding processes were confirmed by computational modelling of this protein structure. These calculations were made by A.Kuznetsov and details of these calculations are described in paper **III**. Shortly, structure of the acrylodan-PKAc adduct was modelled by using MD methods and calculations were made at temperatures 300 K, 500 K and 700 K. In the first case, the structure of the native enzyme was modelled, as shown in Figure 8A. At 700 K complete loss of the protein structure was observed, that exposed the fluorophore in external water medium (Figure 8C). This state is the unfolded protein U, which formation was experimentally documented in this work by the red shift of the fluorescence spectrum of acrylodan, observed at high concentration of chemical denaturants.

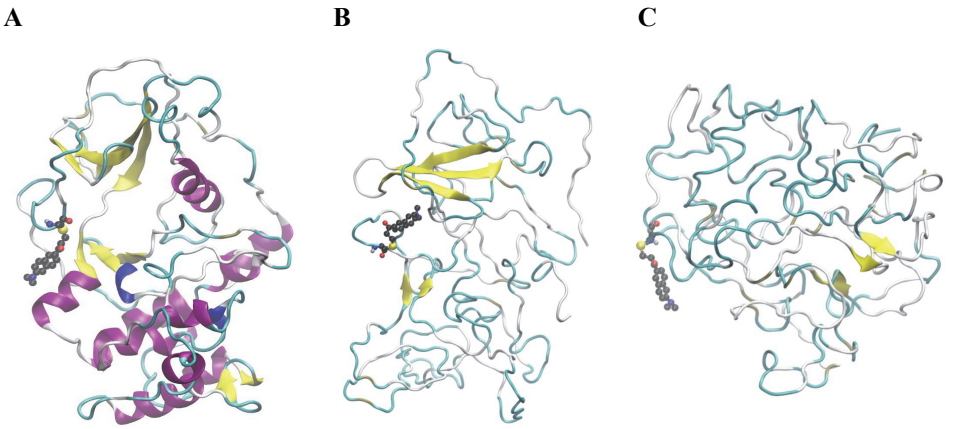

Figure 8. Computer MD modelling of PKAc-acr at 300 K, 500 K and 700 K. **A** MD simulation at 300 K revealed that the structure of PKAc-acr stays intact at this temperature and acrylodan is positioned away from ATP-binding pocket, but is moderately buried in the protein interior and shielded from water molecules. **B** At 500 K structure of PKAc-acr is mostly denatured with few β-sheets still intact. Acrylodan is buried inside the protein interior and shielded from water. **C** At 700 K structure of PKAc-acr is almost fully unfolded, revealing acrylodan to water.

Calculations made at 500 K yielded a protein model, where the main elements of its secondary structure and the hydrophobic core region were still present (Figure 8B). Interestingly, the acrylodan moiety, which is hydrophobic, had shifted towards the hydrophobic core of the protein, in agreement with the blue-shift of its fluorescence spectrum observed in experiments. Following the contemporary models of protein unfolding mechanism, this state could be the "molten globule", which formation is commonly suggested on the protein unfolding path (Baldwin et al., 2010; Malhotra and Udgaonkar, 2016).

However, the results of this study do not allow explicit positioning of this "molten globule" on PKAc unfolding path, as the present experiments do not exclude its formation in parallel with the unfolding step. However, this uncertainty of the molecular mechanism of PKAc denaturation did not hamper application of the denaturation method for ligand binding assay, as under the used conditions only the transfer from N to D state is observed.

4.3. Allostery in PKAc interaction with peptides and nucleotides

4.3.1. Quantification of the allosteric effect

Following the reaction scheme (1), the allosteric effect α can be quantified for any pair of ligands A and B, if the K_a and αK_a or K_b and αK_b values are known. In this work A stands for ATP or any ligand binding in the nucleotide binding site of PKAc, and B is peptide substrate or inhibitor, interacting with the peptide binding site of the enzyme. As seen from the reaction scheme (1), allosteric factor α affects ligand binding regardless of the order the ligands bind to their corresponding binding sites.

For practical determination of α values, interaction of ligands A and B should be studied with the free enzyme E, as well as with the complexes EB and EA, respectively. The experimental method of thermal inactivation kinetic assay, developed in this study, can be used in both cases.

Preliminary experiments, described above, allowed characterization of the enzyme-ligand complex dissociation constants for ATP and peptide inhibitor PKI[5–24], and revealed that simultaneous presence of both ligands resulted in a very strong enhancement of binding effectiveness (Figure 5). This result was in agreement with data, published later by Kim et al (2016), and resulted in the value of the allosteric effect $\alpha = 0.0025$ for this pair of ligands. On the other hand, analysis of other experimental data in literature revealed (Kuznetsov et al., 2009) that α value depends on ligand structure. To specify the nature of this dependence, interaction of a systematic series of peptides with the enzyme was studied (Table 4) and the allosteric effect of ATP was determined. Example of the kinetic assay procedure is shown in Figures 9 and 10.

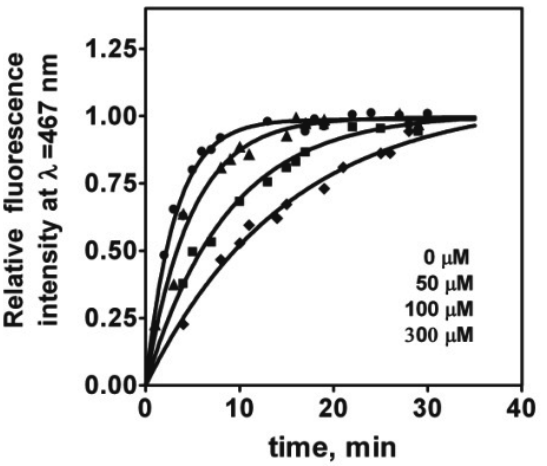

Figure 9. Time course of the fluorescence intensity of the protein-coupled acrylodan, presented as a relative value $\frac{f_t - f_0}{\Delta f_{max}}$, where f_t is fluorescence intensity at time t, f_0 is the fluorescence intensity at t=0, Δf_{max} is the maximal change (span) of the fluorescence intensity, in the absence and presence of inhibitory peptide TGRRNAI-NH_2 at 0 μM (●), 50 μM (▲), 100 μM (■) and 300 μM (♦) concentrations.

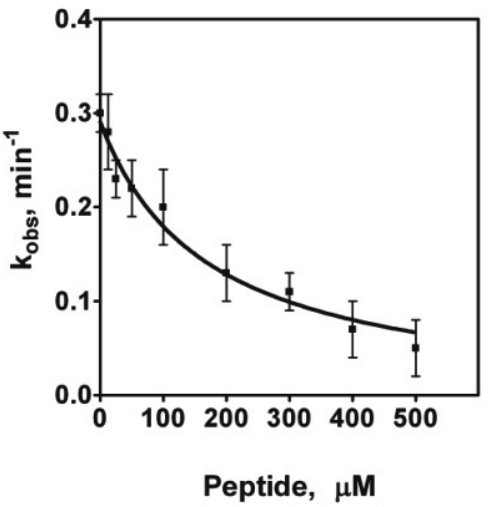

Figure 10. Influence of inhibitory peptide TGRRNAI-NH_2 concentration on rate of PKAc denaturation in 20 mM MOPS buffer (pH 7.0, 10 mM $MgCl_2$, 50 mM NaCl at 25 °C). Enzyme concentration 50 nM.

4.3.2 Influence of peptide structure on allosteric effect of ATP

The proposed method was used to quantify the interaction of series of peptides with the enzyme. These dissociation constants (K_b in Scheme 1) were compared to the K_i values found in literature (Glass et al., 1989), which characterize interaction of these inhibitory peptides with the PKAc – ATP complex (parameters αK_b in Scheme 1). Ratio of these parameters yields the allostery factor α. The results of these experiments are listed in Table 4.

Table 4. Dissociation and inhibitory constants and allosteric factor values for a series of peptides derived from PKI[5–24]

Notation	Peptide structure	K_B, μM	K_i, nM (Glass et al., 1989)	10^3 α
I	TGRRNAI-NH_2	167 ± 39	1900*	8.9
II	GRTLRRNAI-NH_2	85 ± 11	390	4.6
III	DFIASGRTGRRNAI-NH_2	35 ± 9	97	2.8
IV	GRTGRRNAI-NH_2	23 ± 5	36	1.6
V	YADFIASGRTGRRNAI-NH_2	19 ± 4	28	1.5
VI	TTYADFIASGRTGRRNAI-NH_2	8 ± 2	3.1	0.4

* Estimated value from K_i =1250 nM for peptide TGRRNAIHN-NH_2 (Glass et al., 1989)

The allosteric effect depends significantly on peptide structure, and the specificity pattern of peptide recognition by PKAc is similar in the case of the free enzyme and the enzyme-ATP complex. This can be demonstrated by a linear similarity plot comparing the pK_i and pK_b values, as shown in Figure 11. This linear plot includes data points for PKI, which is the parent compound of the studied peptide series and is characterized by the pK_i value of 9.5 (Ashby and Walsh, 1973) and pK_L value of 5.6 (Herberg and Taylor, 1993), and the peptide fragment of this inhibitor protein, denoted as PKI(5–24), which is characterized by the pK_i value 9.7 (Cheng et al., 1985) and pK_L value 5.7 (Masterson et al., 2011a). The latter peptide is a non-amidated analogue of peptide ***VI*** in Table 4 except the missing 2 amino acid residues in C-terminal end.

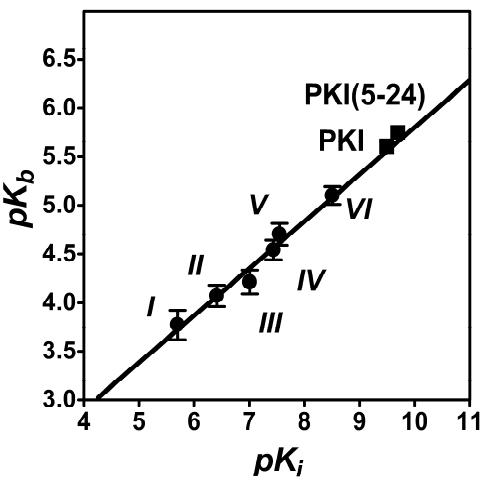

Figure 11. Similarity plot for peptide binding effectiveness with the free enzyme PKAc (pK_L) and its complex with ATP (pK_i). Peptide structures are denoted as in Table 1. Data for PKI and PKI(5–24) were taken from literature. For PKI: pK_i= 9.5 and pK_b= 5.6. For PKI(5–24): pKi= 9.7 and pK_b= 5.7.

Besides this similar specificity pattern, it can be observed that the allosteric effect changes in parallel with peptide affinity, characterized by the K_b values, and this trend can be presented by a linear-free-energy relationship between the pK_b and $p\alpha$ values:

$$p\alpha = C + S\,pK_b \qquad \text{Eq. 6}$$

where C and S stand for the intercept and slope of a linear similarity plot, as shown in Figure 11. In the case of inhibitory peptides ***I–VI***, C = –1.4 ± 0.6 and S = 0.9 ± 0.2. The negative logarithm of the allosteric factor α ($p\alpha$) was used in this similarity plot to emphasize the analogy of this parameter with the traditional pK_b values and to stress the fact that the allosteric effect is presented in the free energy scale.

This similarity plot demonstrates that the same primary structural elements of the peptide sequence govern both the recognition of these ligands in the binding step and the allosteric enhancement of the binding effectiveness, induced by ATP in the present case, and denoted by the $p\alpha$ value. Interestingly, the same kind of similarity plot can also be created for peptide substrates, but it has a different slope (S = 0.42 ± 0.04) (Kuznetsov, Järv, 2008). Therefore, the principle "better binding – stronger allostery" (Kuznetsov and Järv, 2008) holds in the case of peptide inhibitors. Moreover, the same principle is valid also in the case of ATP and its structural analogues such as ADP, adenosine and AMPPNP, which increased the effectiveness of peptide binding with PKAc (Kuznetsov and Järv, 2009), and this increase is again correlated with the binding effectiveness of ligands. Thus, binding effectiveness at both sites is enhanced, and this effect is similar, as the same α value stands in the reaction scheme (1). Moreover, these results demonstrate that interaction between allosterically linked binding sites has no direction, i.e. ligand binding in either one of these sites changes ligand binding effectiveness in the second site and vice versa.

4.3.3 Effect of temperature on ligand binding and allostery

In the following part of this study the kinetic denaturation assay was used to study thermodynamic aspects of the allosteric effect as the assay procedure is applicable for characterization of ligand binding equilibria at different temperatures. Thermodynamic parameters were calculated under conditions where kinetics of the denaturation process could be measured. The results listed in Table 5 for ATP and PKI(5–24), demonstrate that the increase of temperature accelerated overall denaturation rate in all cases, while in the presence of ligands the denaturation rate was slower and the most stable complex was the ternary complex of PKAc, ATP and PKI(5–24). However, this fact did not hinder the analysis, as higher temperatures were used to assay the denaturation

process and the results were presented in coordinates ln k_{obs} vs 1/T, according with the Arrhenius equation:

$$\ln(k) = \ln A - \frac{E_a}{RT} \qquad \text{Eq. 7}$$

It can be seen in Figure 12 that the ln k_{obs} vs 1/T plots were well described by linear interrelationships that allowed estimation of the activation parameters lnA and E_a.

Table 5. Dependence of denaturation rate constants of acrylodan labelled PKAc on temperature in 20 mM MOPS buffer, pH 7.0, 50 mM NaCl, 10 mM $MgCl_2$. Experiments were made in absence or presence of ATP and/or peptide inhibitor PKI[5–24] in the assay medium.

Tempera-ture, °C	k_{obs}, min^{-1}			
	50 nM acr-PKAc	**50 nM acr-PKAc 250 μM ATP**	**50 nM acr-PKAc 1 μM PKI[5–24]**	**50 nM acr-PKAc 250 μM ATP 1 μM PKI[5–24]**
5	0.010 ± 0.003	nd	nd	nd
15	0.090 ± 0.015	0.004 ± 0.001	0.010 ± 0.002	nd
25	0.30 ± 0.04	0.028 ± 0.002	0.06 ± 0.01	nd
30	0.90 ± 0.15	0.12 ± 0.01	0.19 ± 0.02	nd
35	nd	0.37 ± 0.03	0.60 ± 0.06	0.0020 ± 0.0003
40	nd	nd	nd	0.015 ± 0.002
45	nd	nd	nd	0.14 ± 0.01
50	nd	nd	nd	0.67 ± 0.06

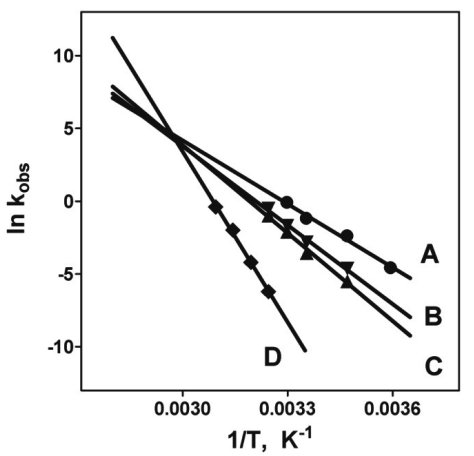

Figure 12. Arrhenius plots for acr-PKAc denaturing. A – 50 nM acr-PKAc, B – 50 nM acr-PKAc + 1 μM PKI[5–24], C – 50 nM acr-PKAc + 250 μM ATP, D – 50 nM acr-PKAc + 250 μM ATP + 1 μM PKI[5–24].

Interestingly, in Figure 12 all the ln(k_{obs}) vs 1/T plots revealed a common intersection point, formally corresponding to the isokinetic temperature of the denaturation reaction. As the existence of this temperature has been debated (Liu and Guo, 2001), it is still hard to connect this phenomenon with some physical process. On the other hand, it is the first time this phenomenon is observed in the case of ligand binding equilibria with enzymes and allosteric interactions between ligand binding sites.

Data from Table 5 was used to calculate K_L and α values for different ligands at different temperatures. Furthermore Van't Hoff equation was applied on those values to calculate the enthalpy and entropy components ΔH and ΔS of the binding process:

$$ln\ K_L = \frac{\Delta H}{RT} - \frac{\Delta S}{R} \qquad \text{(Eq. 8)}$$

In this equation K_L denotes the ligand-protein complex dissociation constant, and ΔH and ΔS are enthalpy and entropy terms, which characterize the ligand-protein interaction, respectively, R is the universal gas constant and T is temperature in Kelvins. Since allostery affects dissociation constants of ligands, we propose that the allosteric factor α can be analyzed by using the same equation (Figure 13B).

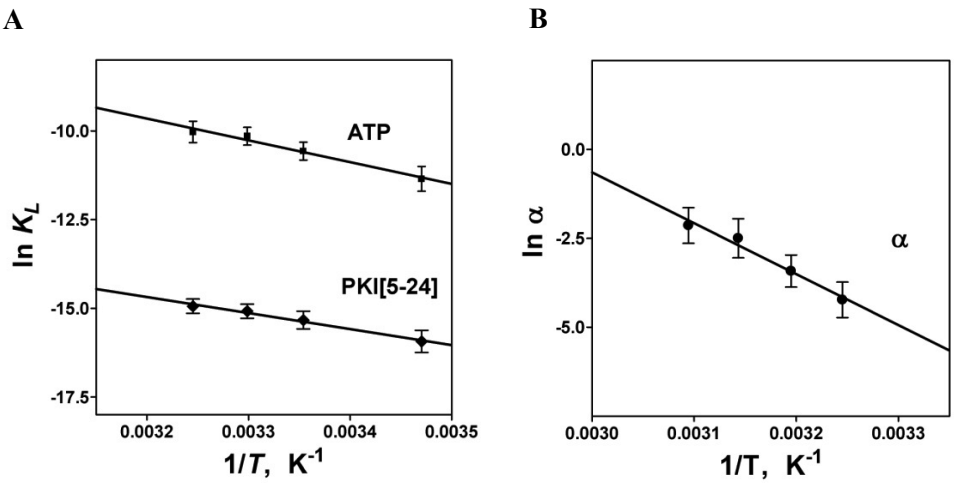

Figure 13. A. Van't Hoff plots for ATP and PKI[5–24] interaction with the acr-PKAc (panel A) and for the allosteric interaction between binding sites of these ligands characterized by α (panel B).

It can be seen from Figure 13A that Van't Hoff equation holds in the case of ATP and inhibitory peptide PKI[5–24] binding, and also, in the case of allostery factor α (Figure 13B). From these plots, thermodynamic parameters characterizing

ligand binding with PKAc were calculated. For ATP $\Delta H = -49 \pm 9$ kJ mol^{-1} and $\Delta S = -78 \pm 19$ J K^{-1} mol^{-1}, for PKI[5–24] $\Delta H = -37 \pm 5$ kJ mol^{-1} and $\Delta S = 5 \pm 9$ J K^{-1} mol^{-1} and for allosteric factor α $\Delta H = -122 \pm 17$ kJ mol^{-1} and $\Delta S = -359 \pm 41$ J K^{-1} mol^{-1}.

These results demonstrate that the allosteric interaction between binding sites is characterized by bigger enthalpy and entropy effects when compared to ligand binding steps. All of these interactions can be presented by a common ΔH vs ΔS plot (Figure 14), pointing to the possibility that ligand binding and allostery are controlled by similar interaction mechanisms. In other words, the same interactions, which govern peptide and nucleotide binding with the protein binding site, are responsible for interaction between these two binding sites. On the other hand, as allosteric effect depends on ligand structure, as demonstrated before, and changes gradually, intensity factors of these interactions should be determined by binding properties of interacting ligands.

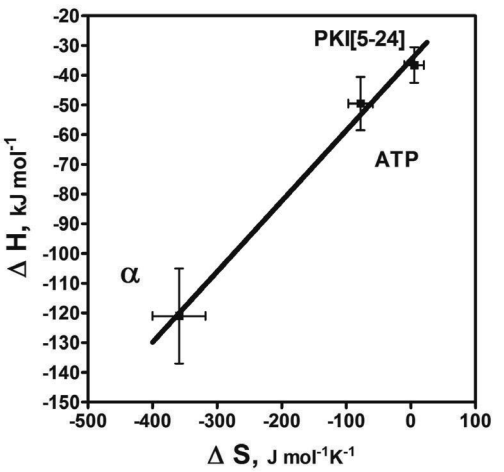

Figure 14. Enthalpy – entropy compensation effect in acr-PKAc interaction with ATP, PKI[5–24] and in allosteric interaction between binding sites for these ligands, quantified by the factor α.

4.3.4 Possible mechanism of the allosteric effect

The results of this study can be used to discuss the thermodynamic aspects of the allosteric effect. It was found that the parameters $\Delta H = -121$ kJ mol^{-1} and $\Delta S = -359$ J K^{-1} mol^{-1} for the allosteric factor α were significantly larger than the entropy and enthalpy changes observed in the case of dissociation of the binary complexes with either ATP or peptide. The negative ΔH value could be linked to formation of new non-covalent bonds in the system, and following the meaning of the parameter α, these interactions should intensify when the ternary complex is formed. The results also indicate that the bonding network changes are accompanied with a large negative entropy change, implying a significant decrease of flexibility of the structure of the ternary complex EAB. It is interesting that there was practically no entropy change during the binary

complex formation with the peptide while the entropy change accompanying ATP binding to PKAc is linked to the enzyme conformational change from open to closed formation (Masterson et al., 2010; Taylor et al., 2004). For binding of PKI[5–24] to PKAc, similar thermodynamic behavior has been reported before (Masterson et al., 2011a). This asymmetric behavior of the enzyme binding sites for nucleotide and peptide ligands may well serve as an additional mechanism, used by the enzyme for amplification of sensitivity of the molecular recognition of peptides via the allosteric effect. If we to take into consideration that in cellular environment average concentration of ATP varies from 1 to 10 mM (Albe et al., 1990), almost all PKAc molecules should be loaded with the nucleotide, as K_d of ATP is around 25 μM. However, for further exploring of this option additional thermodynamic data are needed about interaction of different peptides with the enzyme.

Interestingly, by analogy with the binary complex dissociation, the above-mentioned enthalpy-entropy compensation effect was also observed in the case of the allostery factor, as the negative ΔS and ΔH values compensated each other in calculation of the $\ln K$ value by means of the Van't Hoff equation (6). Therefore, further comparison of the binary and ternary complexes was made in Figure 14, using the ΔS vs ΔH plot. Although the validity of this type of analysis has been discussed from different points of view (Liu and Guo, 2001), it is accepted that the linear interrelationship between the ΔS and ΔH values for different processes could still implicate the presence of a common (or dominant) mechanism within this group of processes. In this case the correlated processes were the binary complex dissociation on the one hand, and the allosteric interaction between the two binding sites on the other hand. The linear-free-energy relationship between the binding effectiveness of peptide substrates (pK_B) and the allosteric effect ($p\alpha$), leading to formulation of the principle "better binding – stronger allostery" (Kuznetsov and Järv, 2008a), can be taken as a good example of this type of inter-relationship.

Moreover, the conclusion that the allosteric effect and ligand binding effectiveness could be governed by similar mechanism, and therefore, depend on structure of both peptide and nucleotide ligands, is a clear indication that the allosteric interaction between the two binding sites cannot be explained proceeding from the existence of some fixed network of interactions between certain components of the protein structure. Most probably, these interactions could be explained by formation of conformational ensembles, which take into consideration the specific features of the binding site as well as structure of the ligand, and enable in this way the amplification of the enzyme specificity.

The linear interrelationship between the pK_b and $p\alpha$ values (and also between pK_A and $p\alpha$ values in Scheme 1) demonstrates that the same specificity factors govern binding effectiveness and the allosteric effect in the case of the same ligand. This means that allostery does not add new interatomic interactions between the ligand and its binding site, but rather changes the intensity (or "firmness") of the existing interactions. In the case of the studied peptide

inhibitors, the increase in binding energy is rather significant, altering the dissociation constant by up to 4 orders of magnitude.

To explain these phenomena, it is important to understand that the effectiveness of ligand binding is governed by the ratio of its off-rate and on-rate constants, and that alteration of one of these parameters is sufficient to change the dissociation constant of the ligand-protein complex and the free energy of the binding process. If ligand association with a protein can be considered as a diffusion-controlled process, where the protein molecule has a negligible role (Shoup and Szabo, 1982), attention should be focused on the ligand off-rate and the interrelationship between the ligand-protein complex dissociation rate and ligand binding affinity.

Ligand binding effectiveness is governed by interactions between this molecule and the amino acid residues in the protein ligand binding site, and these interactions are the main driving force of molecular recognition. However, kinetic studies have revealed that the off-rate (or ligand residence time in the binding site) can be modulated by the intrinsic dynamics of the protein, as its movements are important for ligand "roll out" from the binding site (Carroll et al, 2012). This means that the "opening rate" of the binding site could significantly govern the release of the protein-bound ligand, and the ligand off-rate, as well as affinity should be similarly modulated by the intrinsic dynamics of protein structure. For PKAc, the limiting step in catalysis is the release of ADP from the nucleotide binding pocket (Zhou and Adams, 1997). There are plenty of evidence that protein dynamics is changed by ligand binding, and that these changes affect a rather large proportion, if not the whole protein molecule (Henzler-Wildman and Kern, 2007; Masterson et al., 2008, 2011a). The same phenomenon explains the well-known fact that proteins are stabilized in the presence of specific ligands, which has been used for the development of the denaturation assay of ligand-protein complex formation and is the basis for the experiments made in this study.

These two well-known facts – the regulation of the ligand off-rate by protein intrinsic dynamics, and the alteration of the protein's intrinsic dynamics by ligand binding – may be the key elements of the operational mechanism of allostery. Following this hypothesis, the allosteric regulation of enzyme affinity may be caused by alteration of the ligand off-rate from the binding site, governed by the dynamic properties of the protein. On the other hand, protein dynamics are governed by the binding of specific ligand(s). If the extent of the change in dynamics is correlated with the overall energy of ligand binding, this mechanism explains the cumulative effect of different ligands on allostery ($p\alpha$), and also justifies the principle "better binding – stronger allostery". Furthermore, the interatomic forces between the ligand molecule and amino acid residues in its binding site are still responsible for ligand recognition and manifestation of the classical specificity pattern.

The effect of protein stabilization on ligand binding effectiveness cannot be experimentally revealed in the case of binding of a single molecule, but if this binding can be studied in the absence and in the presence of another ligand,

which also affects protein dynamics, this effect can be easily quantified, as was done in the present study.

The fact that ligand binding effectiveness (or the residence time in its binding site) could be governed by protein intrinsic dynamics, and that this protein property may govern binding of other ligands in distinct binding sites, may have a crucial influence on our understanding of regulation phenomena in various biological processes. The most exciting aspect of this explanation is that there is no need for specific “relay” structures for transmission of allosteric effects between two related sites, but the alteration of binding effectiveness, described in terms of allostery, may be triggered by the binding of a ligand in a remote binding site, where it can still affect the dynamic state of the protein molecule, as was theoretically modeled by Cooper and Dryden in 1984 (Cooper and Dryden, 1984). This principle expands our understandings about allosteric regulation and could lead to discovery of alternative possibilities for the design of allosterically interacting drugs.

CONCLUSIONS

1. Mutation of PKAc at position N326 to C and subsequent labelling of the protein with acrylodan, which is a fluorophore that is sensitive to its microenvironment, proved to be a useful tool to study ligand binding using a novel method that utilizes fluorescence change that accompanies protein denaturation in time dependent manner.
2. The sensitive dependence of fluorescence change rate on ligand concentration allowed to assess binding affinities for both ATP-binding pocket and peptide binding site targeting molecules. To assess ligand binding affinity, a measurement of PKAc-acr denaturation in the absence and presence of ligand were performed and the ratio between denaturation rates was calculated. This ratio is proportional to the ratio of ligand concentration and its binding affinity. As only two measurements have to be performed in absence and presence of a ligand, it could potentially be a useful method to be used in high-throughput ligand binding assays.
3. Experiments, where urea or guanidine hydrochloride were used as denaturants, revealed 3 different structural states for PKAc-acr: 1) native (or active) 2) denatured and 3) unfolded. As these different structural states had different fluorescence characteristics, it was concluded that acrylodan moiety changed its relative position in the protein structure and this was reflected in changes to its microenvironment. This hypothesis was confirmed by computer modelling of PKAc-acr unfolding at different temperatures.
4. Thermodynamic parameters, which characterize binding of ATP and peptide inhibitor PKI(5–24) with the enzyme and also the allosteric interaction between these binding sites, revealed that ligand binding and allosteric effect are probably governed by similar interaction mechanisms. It was also revealed that nucleotide and inhibitory peptide binding have different enthalpic and entropic contributions, pointing to different influence that these ligands have on protein structure after binding. While peptide inhibitor binding is governed mainly by enthalpy and therefore formation of novel non-covalent bonds between peptide and protein binding site can be expected, ATP binding had both enthalpic and entropic components in its binding, pointing to formation of novel non-covalent bonds and reduction of PKAc backbone flexibility. Thermodynamic parameters for allosteric effect revealed that both enthalpy and entropy had larger influence on for allosteric effect when compared to ligand binding parameters. It can be concluded, that the interplay between ligand binding sites have much greater effect to the protein structure than binding of both ligands separately.
5. Allosteric effect of ATP on binding of series of congeneric inhibitory peptides with PKAc depends on peptide structure and comparison of these data with effectiveness of peptide binding with the free enzyme revealed that both phenomena are governed by the same specificity determining factors. There-

fore, the principle “better binding – stronger allostery” can be observed in the case of this series of peptide inhibitors.

6. The influence of ligand binding on intrinsic dynamics of the protein molecule may be responsible for allosteric phenomena, observed in the case of simultaneous binding of two ligands with one protein, while the observed effect of allostery is governed cumulatively by binding effectiveness of both molecules.

SUMMARY

In this work, the acrylodan labelled N326C PKAc was prepared and its fluorescence properties were studied in the presence of different chemical denaturants. As fluorescence of this dye is sensitive to the conformational changes of the protein, this phenomenon was used to develop a denaturation kinetics assay for detection of ligand binding to PKAc. This assay procedure is universal and does not depend on type of ligand. The proposed assay was applied for quantification of allosteric effect of ligands, which interact with either nucleotide or peptide binding site of the enzyme, and also for analysis of the thermodynamic and extra-thermodynamic aspects of this interaction.

The fluorescence spectra of PKAc-acr adduct were also analyzed to study the kinetic mechanism of unfolding of this protein in the presence of chemical denaturants (urea, guanidine hydrochloride and MOPS). These studies revealed that three different states of the protein can be differentiated by fluorescence measurements, defined as native, denatured and unfolded structures. It was suggested that the denatured state corresponds to the molten globule structure of the protein. These conclusions were confirmed by results of computational modelling of the protein-dye adduct structure.

Equilibria of protein-ligand complex formation were studied at different temperatures and thermodynamic parameters ΔH and ΔS were determined for PKAc interaction with ATP and peptide inhibitor PKI(5–24), as well as for allosteric enhancement of binding effectiveness of these ligands in the ternary complex. It was concluded that binding effectiveness and allosteric effect are governed by similar interactions, and in the case of allosteric effect significant change of entropy is observed. The latter fact points to the possibility that in the presence of two ligands the intrinsic dynamics of the protein molecule is strongly reduced that may play an important role in allosteric enhancement of ligand binding effectiveness.

Allosteric effect of ATP was studied on binding of a series of peptide inhibitors with the enzyme. The results of this analysis revealed that this effect depends on peptide structure and it is governed by the same specificity factors as the peptide binding effectiveness. This phenomenon follows the principle „better binding – stronger allostery“, and is in agreement with the possibility that allosteric enhancement of binding effectiveness is not caused by formation of additional interactions between the binding site and ligand molecule, but rather reflects gradual modulation of interactions, which are responsible for molecular recognition of the ligand molecule in the binding site of the free enzyme.

SUMMARY IN ESTONIAN

cAMP-sõltuva proteiinkinaasi katalüütilise alaühiku allosteerika

Antud doktoritöö käigus valmistati akrülodaniga märgistatud PKAc N326C ja uuriti selle fluorestsentsi omadusi erinevate keemiliste denaturantide juuresolekul. Kuna selle värvaine fluorestsents on tundlik valgu konformatsiooniliste muutuste suhtes, kasutati seda nähtust, et välja töötada denatureeriva kineetika meetod ligandi sidumise määramiseks PKAc-ga. See analüüsimeetod on universaalne ja ei sõltu ligandi tüübist. Meetodit kasutati nukleotiidsete või peptiidligandide allosteerilise efekti kvantifitseerimiseks ning nende interaktsioonide termodünaamiliste ja ekstra-termodünaamiliste aspektide analüüsimiseks.

Analüüsiti ka akrülodaaniga seotud PKAc fluorestsentspektreid, et uurida selle valgu denatureerimise kineetilisi mehhanisme keemiliste denaturantide (uurea, guanidiinvesinikkloriid ja MOPS) juuresolekul. Need uuringud näitasid, et fluorestsentsmõõtmiste abil saab valgul eristada kolme erinevat seisundit: natiivne ehk aktiivne, denatureerunud ja struktuuritu. Katsete tulemusena jõuti järeldusele, et denatureeritud olek vastab valgu sulaglobuli struktuurile. Neid järeldusi kinnitas märgistatud valgu fluorestsentsspektrite arvutuslik modelleerimine.

Erinevatel temperatuuridel määrati PKAc – ATP ja PKAc – peptiidinhibiitoriga PKI[5–24] valk-ligandi komplekside moodustamise tasakaalulised väärtused ja arvutati nende nähtuste termodünaamilised parameetrid ΔH ja ΔS. Leiti, et nii ligandi sidumise kui ka allosteerilise efekti tekkemehhanism põhineb samadel alustel. Allosteerilise efekti korral täheldatakse märkimisväärset entroopia vähenemist. Viimane asjaolu viitab võimalusele, et kahe ligandi juuresolekul on valgumolekuli dünaamika tugevalt vähenenud, mis võib mängida olulist rolli ligandi siduvuse efektiivsuse allosteerilises parandamises.

ATP allosteerilist toimet uuriti ensüümiga sidumisel koosmõjus rea peptiidsete inhibiitoritega. Mõõtmistulemused näitasid, et allosteeriline toime sõltub peptiidi struktuurist ja et seda reguleerivad samad spetsiifilisusfaktorid nagu peptiidi sidumiselgi. Allosteerika nähtus järgib põhimõtet "mida parem ligandi siduvus, seda tugevam allosteerika" ning on kooskõlas võimalusega, et sidumisvõime allosteeriline võimendamine ei ole tingitud seondumiskoha ja ligandi molekuli vahelistest täiendavatest interaktsioonidest, vaid peegeldab vastastikmõju järkjärgulist modulatsiooni, mis vastutavad vaba ensüümi seondumiskohas ligandi molekulaarse äratundmise eest.

ACKNOWLEDGEMENTS

First and foremost I would like to express my sincerest gratitude to my supervisor prof. Jaak Järv for his guidance and wisdom in the field of science aswell as life throughout the years. I admire your everlasting optimism and ability to figure out patterns from loads of data.

I would like to thank prof. Mart Loog for his guidance, support and opportunity to work in his lab on interesting projects.

Special thanks to dr. Per Jemth from Uppsala University for the opportunity to visit his lab and use the equipment for performing experiments.

I'm also grateful to all of the co-authors of my papers, namely Piret Arukuusk, Tõiv Haljasorg, Aleksei Kuznetsov and Karina Solovjova, for their work and helpful comments on the manuscripts. Special thanks to Meeme Utt for his help.

Many thanks to Siim Kukk, Anu Ploom and Siim Salmar for helpful comments on the manuscript.

I'm grateful to my colleagues Ervin, Rainis, Ilona, Mihkel, Kaidi and all the other folks at Loog lab for making working fun and interesting. Our discussions about everything imaginable have been great!

My fellow coursemates Lari, Peeter, Marit, Kadri, Tiit, Mari and Andres – thanks, it has been fun.

My longtime friends Arko, Priit, Siim, Ott, Pille, Priit, Hedi-Liis, Fred, Mats – thanks for the fun times!

I wish to thank my family, especially my mother Hille and sister Triin, for believing in and supporting me throughout all those years.

My dearest Kersti – thank you for your everlasting support and love! You, our son Torm and dog Staut make my world immensely richer and more satisfying.

REFERENCES

Albe, K.R., Butler, M.H., and Wright, B.E. (1990). Cellular concentrations of enzymes and their substrates. J. Theor. Biol. *143*, 163–195.

de Araujo, E.D., Manaswiyoungkul, P., Israelian, J., Park, J., Yuen, K., Farhangi, S., Berger-Becvar, A., Abu-Jazar, L., and Gunning, P.T. (2017). High-throughput thermofluor-based assays for inhibitor screening of STAT SH2 domains. J. Pharm. Biomed. Anal. *143*, 159–167.

Ashby, C.D., and Walsh, D.A. (1973). Characterization of the Interaction of a Protein Inhibitor with Adenosine 3',5'-Monophosphate-dependent Protein Kinases II. MECHANISM OF ACTION WITH THE HOLOENZYME. J. Biol. Chem. *248*, 1255–1261.

Bacalum, M., Zorilă, B., and Radu, M. (2013). Fluorescence spectra decomposition by asymmetric functions: Laurdan spectrum revisited. Anal. Biochem. *440*, 123–129.

Baldwin, R.L., Frieden, C., and Rose, G.D. (2010). Dry Molten Globule Intermediates and the Mechanism of Protein Unfolding. Proteins *78*, 2725–2737.

Burnett, G., and Kennedy, E.P. (1954). The Enzymatic Phosphorylation of Proteins. J. Biol. Chem. *211*, 969–980.

Cheng, H.C., van Patten, S.M., Smith, A.J., and Walsh, D.A. (1985). An active twenty-amino-acid-residue peptide derived from the inhibitor protein of the cyclic AMP-dependent protein kinase. Biochem. J. *231*, 655–661.

Cohen, P. (2001). The role of protein phosphorylation in human health and disease. Eur. J. Biochem. *268*, 5001–5010.

Corbin, J.D., Sugden, P.H., West, L., Flockhart, D.A., Lincoln, T.M., and McCarthy, D. (1978). Studies on the properties and mode of action of the purified regulatory subunit of bovine heart adenosine 3':5'-monophosphate-dependent protein kinase. J. Biol. Chem. *253*, 3997–4003.

Ducommun, B., Brambilla, P., Félix, M.A., Franza, B.R., Karsenti, E., and Draetta, G. (1991). cdc2 phosphorylation is required for its interaction with cyclin. EMBO J. *10*, 3311–3319.

Emel'ianenko, V.I., Reshetniak, I.K., Andreev, O.A., and Burshteĭn, E.A. (2000). [Analysis of log-normal components of fluorescence spectra of prodan and acrylodan bound to proteins]. Biofizika *45*, 207–219.

Esseltine, J.L., and Scott, J.D. (2013). AKAP signaling complexes: pointing towards the next generation of therapeutic targets? Trends Pharmacol. Sci. *34*, 648–655.

Fang, Y. (2012). Ligand-receptor interaction platforms and their applications for drug discovery. Expert Opin. Drug Discov. *7*, 969–988.

Glass, D.B., Cheng, H.C., Mende-Mueller, L., Reed, J., and Walsh, D.A. (1989). Primary structural determinants essential for potent inhibition of cAMP-dependent protein kinase by inhibitory peptides corresponding to the active portion of the heat-stable inhibitor protein. J. Biol. Chem. *264*, 8802–8810.

Henzler-Wildman, K., and Kern, D. (2007). Dynamic personalities of proteins. Nature *450*, 964–972.

Herberg, F.W., and Taylor, S.S. (1993). Physiological inhibitors of the catalytic subunit of cAMP-dependent protein kinase: effect of MgATP on protein-protein interactions. Biochemistry (Mosc.) *32*, 14015–14022.

Johnson, D.A., Akamine, P., Radzio-Andzelm, E., Madhusudan, and Taylor, S.S. (2001). Dynamics of cAMP-Dependent Protein Kinase. Chem. Rev. *101*, 2243–2270.

Kim, J., Li, G., Walters, M.A., Taylor, S.S., and Veglia, G. (2016). Uncoupling Catalytic and Binding Functions in the Cyclic AMP-Dependent Protein Kinase A. Structure *24*, 353–363.

Knighton, D.R., Zheng, J.H., Eyck, L.T., Ashford, V.A., Xuong, N.H., Taylor, S.S., and Sowadski, J.M. (1991a). Crystal structure of the catalytic subunit of cyclic adenosine monophosphate-dependent protein kinase. Science *253*, 407–414.

Knighton, D.R., Zheng, J.H., Eyck, L.T., Xuong, N.H., Taylor, S.S., and Sowadski, J.M. (1991b). Structure of a peptide inhibitor bound to the catalytic subunit of cyclic adenosine monophosphate-dependent protein kinase. Science *253*, 414–420.

Kõivomägi, M., Valk, E., Venta, R., Iofik, A., Lepiku, M., Balog, E.R.M., Rubin, S.M., Morgan, D.O., and Loog, M. (2011). Cascades of multisite phosphorylation control Sic1 destruction at the onset of S phase. Nature *480*, 128–131.

Kornev, A.P., Taylor, S.S., and Eyck, L.F.T. (2008). A helix scaffold for the assembly of active protein kinases. Proc. Natl. Acad. Sci. *105*, 14377–14382.

Kuznetsov, A., and Järv, J. (2008a). Allosteric Cooperativity in Inhibition of Protein Kinase a Catalytic Subunit. Open Enzyme Inhib. J. *1*.

Kuznetsov, A., and Järv, J. (2008b). Single-subunit allostery in the kinetics of peptide phosphorylation by protein kinase A. Proc. Est. Acad. Sci. *57*, 247.

Lew, J., Coruh, N., Tsigelny, I., Garrod, S., and Taylor, S.S. (1997a). Synergistic Binding of Nucleotides and Inhibitors to cAMP-dependent Protein Kinase Examined by Acrylodan Fluorescence Spectroscopy. J. Biol. Chem. *272*, 1507–1513.

Lew, J., Taylor, S.S., and Adams, J.A. (1997b). Identification of a Partially Rate-Determining Step in the Catalytic Mechanism of cAMP-Dependent Protein Kinase: A Transient Kinetic Study Using Stopped-Flow Fluorescence Spectroscopy. Biochemistry (Mosc.) *36*, 6717–6724.

Li, Y., and Kang, C. (2017). Solution NMR Spectroscopy in Target-Based Drug Discovery. Molecules *22*, 1399.

Liku, M.E., Nguyen, V.Q., Rosales, A.W., Irie, K., and Li, J.J. (2005). CDK phosphorylation of a novel NLS-NES module distributed between two subunits of the Mcm2-7 complex prevents chromosomal rereplication. Mol. Biol. Cell *16*, 5026–5039.

Liu, L., and Guo, Q.-X. (2001). Isokinetic Relationship, Isoequilibrium Relationship, and Enthalpy−Entropy Compensation. Chem. Rev. *101*, 673–696.

Mahendrarajah, K., Dalby, P.A., Wilkinson, B., Jackson, S.E., and Main, E.R.G. (2011). A high-throughput fluorescence chemical denaturation assay as a general screen for protein–ligand binding. Anal. Biochem. *411*, 155–157.

Malhotra, P., and Udgaonkar, J.B. (2016). How cooperative are protein folding and unfolding transitions? Protein Sci. *25*, 1924–1941.

Manning, G., Whyte, D.B., Martinez, R., Hunter, T., and Sudarsanam, S. (2002). The protein kinase complement of the human genome. Science *298*, 1912–1934.

Masterson, L.R., Mascioni, A., Traaseth, N.J., Taylor, S.S., and Veglia, G. (2008). Allosteric cooperativity in protein kinase A. Proc. Natl. Acad. Sci. *105*, 506–511.

Masterson, L.R., Cheng, C., Yu, T., Tonelli, M., Kornev, A., Taylor, S.S., and Veglia, G. (2010). Dynamics connect substrate recognition to catalysis in protein kinase A. Nat. Chem. Biol. *6*, 821–828.

Masterson, L.R., Shi, L., Metcalfe, E., Gao, J., Taylor, S.S., and Veglia, G. (2011a). Dynamically committed, uncommitted, and quenched states encoded in protein kinase A revealed by NMR spectroscopy. Proc. Natl. Acad. Sci. *108*, 6969–6974.

Masterson, L.R., Yu, T., Shi, L., Wang, Y., Gustavsson, M., Mueller, M.M., and Veglia, G. (2011b). cAMP-Dependent Protein Kinase A Selects the Excited State of the Membrane Substrate Phospholamban. J. Mol. Biol. *412*, 155–164.

Monod, J., Wyman, J., and Changeux, J.P. (1965). ON THE NATURE OF ALLOSTERIC TRANSITIONS: A PLAUSIBLE MODEL. J. Mol. Biol. *12*, 88–118.

Nussinov, R., and Tsai, C.-J. (2013). Allostery in Disease and in Drug Discovery. Cell *153*, 293–305.

Prendergast, F.G., Meyer, M., Carlson, G.L., Iida, S., and Potter, J.D. (1983). Synthesis, spectral properties, and use of 6-acryloyl-2-dimethylaminonaphthalene (Acrylodan). A thiol-selective, polarity-sensitive fluorescent probe. J. Biol. Chem. *258*, 7541–7544.

Roskoski Jr., R. (2015). A historical overview of protein kinases and their targeted small molecule inhibitors. Pharmacol. Res. *100*, 1–23.

Senisterra, G., Chau, I., and Vedadi, M. (2011). Thermal Denaturation Assays in Chemical Biology. ASSAY Drug Dev. Technol. *10*, 128–136.

Siano, D.B., and Metzler, D.E. (1969). Band Shapes of the Electronic Spectra of Complex Molecules. J. Chem. Phys. *51*, 1856–1861.

Simard, J.R., Grütter, C., Pawar, V., Aust, B., Wolf, A., Rabiller, M., Wulfert, S., Robubi, A., Klüter, S., Ottmann, C., et al. (2009). High-throughput screening to identify inhibitors which stabilize inactive kinase conformations in p38alpha. J. Am. Chem. Soc. *131*, 18478–18488.

Taylor, S.S., Yang, J., Wu, J., Haste, N.M., Radzio-Andzelm, E., and Anand, G. (2004). PKA: a portrait of protein kinase dynamics. Biochim. Biophys. Acta BBA – Proteins Proteomics *1697*, 259–269.

Taylor, S.S., Ilouz, R., Zhang, P., and Kornev, A.P. (2012a). Assembly of allosteric macromolecular switches: lessons from PKA. Nat. Rev. Mol. Cell Biol. *13*, 646–658.

Taylor, S.S., Keshwani, M.M., Steichen, J.M., and Kornev, A.P. (2012b). Evolution of the eukaryotic protein kinases as dynamic molecular switches. Phil Trans R Soc B *367*, 2517–2528.

Tsai, C.-J., and Nussinov, R. (2014). A Unified View of "How Allostery Works." PLOS Comput. Biol. *10*, e1003394.

Vedadi, M., Niesen, F.H., Allali-Hassani, A., Fedorov, O.Y., Finerty, P.J., Wasney, G.A., Yeung, R., Arrowsmith, C., Ball, L.J., Berglund, H., et al. (2006). Chemical screening methods to identify ligands that promote protein stability, protein crystallization, and structure determination. Proc. Natl. Acad. Sci. *103*, 15835–15840.

Wada, A., Mie, M., Aizawa, M., Lahoud, P., Cass, A.E.G., and Kobatake, E. (2003). Design and Construction of Glutamine Binding Proteins with a Self-Adhering Capability to Unmodified Hydrophobic Surfaces as Reagentless Fluorescence Sensing Devices. J. Am. Chem. Soc. *125*, 16228–16234.

Walsh, D.A., Perkins, J.P., and Krebs, E.G. (1968). An Adenosine 3',5'-Monophosphate-dependant Protein Kinase from Rabbit Skeletal Muscle. J. Biol. Chem. *243*, 3763–3765.

Whitehouse, S., and Walsh, D.A. (1983). Mg X ATP2-dependent interaction of the inhibitor protein of the cAMP-dependent protein kinase with the catalytic subunit. J. Biol. Chem. *258*, 3682–3692.

Whitehouse, S., Feramisco, J.R., Casnellie, J.E., Krebs, E.G., and Walsh, D.A. (1983). Studies on the kinetic mechanism of the catalytic subunit of the cAMP-dependent protein kinase. J. Biol. Chem. *258*, 3693–3701.

Zheng, J., Knighton, D.R., ten Eyck, L.F., Karlsson, R., Xuong, N., Taylor, S.S., and Sowadski, J.M. (1993). Crystal structure of the catalytic subunit of cAMP-dependent protein kinase complexed with MgATP and peptide inhibitor. Biochemistry (Mosc.) *32*, 2154–2161.

Zhou, J., and Adams, J.A. (1997). Participation of ADP Dissociation in the Rate-Determining Step in cAMP-Dependent Protein Kinase. Biochemistry (Mosc.) *36*, 15733–15738.

PUBLICATIONS

CURRICULUM VITAE

Name: Rait Kivi
Date of birth: November 18, 1984
Address: Institute of Chemistry, Ravila 14a, 50411, Tartu, Estonia
Nationality: Estonian
E-mail: rait.kivi@ut.ee

Education

2010–... University of Tartu, doctorial studies (Chemistry)
2008–2010 University of Tartu, MSc (Gene technology)
2005–2008 University of Tartu, BSc (Gene technology)
1992–2004 Saaremaa's Co-ed Gymnasium

Professional employment

2016–... University of Tartu, Institute of Technology, Junior Researcher
2014–2015 University of Tartu, Institute of Chemistry, Junior Researcher
2012–2013 University of Tartu, Institute of Chemistry, chemist

Scientific publications

1. Kuznetsov, Aleksei; **Kivi, Rait**; Järv, Jaak (2016). Computational modeling of acrylodan-labeled cAMP-dependent protein kinase catalytic subunit unfolding. Computational Biology and Chemistry, 61, 197−201.10.1016/j.compbiolchem.2016.01.004.
2. **Kivi, Rait**; Järv, Jaak (2016). Different States of Acrylodan-Labeled 3'5'-Cyclic Adenosine Monophosphate Dependent Protein Kinase Catalytic Subunits in Denaturant Solutions. The protein journal, 35 (5), 331−339.
3. **Kivi, Rait**; Solovjova, Karina; Haljasorg, Tõiv; Arukuusk, Piret; Järv, Jaak (2016). Allosteric Effect of Adenosine Triphosphate on Peptide Recognition by 3'5'-Cyclic Adenosine Monophosphate Dependent Protein Kinase Catalytic Subunits. The protein journal, 35 (6), 459−466.
4. **Kivi, Rait**; Jemth, Per; Järv, Jaak (2014). Thermodynamic aspects of cAMP dependent protein kinase catalytic subunit allostery. The Protein Journal, 33 (4), 393−396.
5. **Kivi, Rait**; Loog, Mart; Jemth, Per; Järv, Jaak (2013). Kinetics of Acrylodan-Labelled cAMP-Dependent Protein Kinase Catalytic Subunit Denaturation. The Protein Journal, 32 (7), 519−525.10.1007/s10930-013-9511-4.
6. Kõivomägi, Mardo; Örd, Mihkel; Iofik, Anna; Valk, Ervin; Venta, Rainis; Faustova, Ilona; **Kivi, Rait**; Balog, Eva Rose M; Rubin, Seth M; Loog, Mart (2013). Multisite phosphorylation networks as signal processors for Cdk1. Nature Structural & Molecular Biology, 1415−1424.10.1038/nsmb.2706.

7. Timasheva, Yanina; Putku, Margus; **Kivi, Rait**; Kožich, Viktor; Männik, Jaana; Laan, Maris (2013). Developmental programming of growth: Genetic variant in GH2 gene encoding placental growth hormone contributes to adult height determination. Placenta, 34 (11), 995−1001.10.1016/j.placenta.2013.08.012.
8. Kivistik, Paula Ann.; **Kivi, Rait**; Kivisaar, Maia; Hõrak, Rita (2009). Identification of ColR binding consensus and prediction of regulon of ColRS two-component system. BMC Molecular Biology, 10 (46), 1−13.

ELULOOKIRJELDUS

Nimi: Rait Kivi
Sünniaeg: November 18, 1984
Aadress: Keemia instituut, Ravila 14a, 50411, Tartu, Eesti
Kodakondsus: Eesti
E-post: rait.kivi@ut.ee

Hariduskäik

2010–... Tartu Ülikool, doktoriõpe (Keemia)
2008–2010 Tartu Ülikool, MSc (Geenitehnoloogia)
2005–2008 Tartu Ülikool BSc (Geenitehnoloogia)
1992–2004 Saaremaa Ühisgümnaasium

Teenistuskäik

2016–... Tartu Ülikool, Tehnoloogiainstituut, nooremteadur
2014–2015 Tartu Ülikool, Keemia instituut, nooremteadur
2012–2013 Tartu Ülikool, Keemia instituut, keemik

Teaduspublikatsioonid

1. Kuznetsov, Aleksei; **Kivi, Rait**; Järv, Jaak (2016). Computational modeling of acrylodan-labeled cAMP-dependent protein kinase catalytic subunit unfolding. Computational Biology and Chemistry, 61, 197−201.10.1016/j.compbiolchem.2016.01.004.
2. **Kivi, Rait**; Järv, Jaak (2016). Different States of Acrylodan-Labeled 3'5'-Cyclic Adenosine Monophosphate Dependent Protein Kinase Catalytic Subunits in Denaturant Solutions. The protein journal, 35 (5), 331−339.
3. **Kivi, Rait**; Solovjova, Karina; Haljasorg, Tõiv; Arukuusk, Piret; Järv, Jaak (2016). Allosteric Effect of Adenosine Triphosphate on Peptide Recognition by 3'5'-Cyclic Adenosine Monophosphate Dependent Protein Kinase Catalytic Subunits. The protein journal, 35 (6), 459−466.
4. **Kivi, Rait**; Jemth, Per; Järv, Jaak (2014). Thermodynamic aspects of cAMP dependent protein kinase catalytic subunit allostery. The Protein Journal, 33 (4), 393−396.
5. **Kivi, Rait**; Loog, Mart; Jemth, Per; Järv, Jaak (2013). Kinetics of Acrylodan-Labelled cAMP-Dependent Protein Kinase Catalytic Subunit Denaturation. The Protein Journal, 32 (7), 519−525.10.1007/s10930-013-9511-4.
6. Kõivomägi, Mardo; Örd, Mihkel; Iofik, Anna; Valk, Ervin; Venta, Rainis; Faustova, Ilona; **Kivi, Rait**; Balog, Eva Rose M; Rubin, Seth M; Loog, Mart (2013). Multisite phosphorylation networks as signal processors for Cdk1. Nature Structural & Molecular Biology, 1415−1424.10.1038/nsmb.2706.

7. Timasheva, Yanina; Putku, Margus; **Kivi, Rait**; Kožich, Viktor; Männik, Jaana; Laan, Maris (2013). Developmental programming of growth: Genetic variant in GH2 gene encoding placental growth hormone contributes to adult height determination. Placenta, 34 (11), 995−1001.10.1016/j.placenta.2013.08.012.
8. Kivistik, Paula Ann.; **Kivi, Rait**; Kivisaar, Maia; Hõrak, Rita (2009). Identification of ColR binding consensus and prediction of regulon of ColRS two-component system. BMC Molecular Biology, 10 (46), 1−13.

DISSERTATIONES CHIMICAE UNIVERSITATIS TARTUENSIS

1. **Toomas Tamm.** Quantum-chemical simulation of solvent effects. Tartu, 1993, 110 p.
2. **Peeter Burk.** Theoretical study of gas-phase acid-base equilibria. Tartu, 1994, 96 p.
3. **Victor Lobanov.** Quantitative structure-property relationships in large descriptor spaces. Tartu, 1995, 135 p.
4. **Vahur Mäemets.** The ^{17}O and ^{1}H nuclear magnetic resonance study of H_2O in individual solvents and its charged clusters in aqueous solutions of electrolytes. Tartu, 1997, 140 p.
5. **Andrus Metsala.** Microcanonical rate constant in nonequilibrium distribution of vibrational energy and in restricted intramolecular vibrational energy redistribution on the basis of slater's theory of unimolecular reactions. Tartu, 1997, 150 p.
6. **Uko Maran.** Quantum-mechanical study of potential energy surfaces in different environments. Tartu, 1997, 137 p.
7. **Alar Jänes.** Adsorption of organic compounds on antimony, bismuth and cadmium electrodes. Tartu, 1998, 219 p.
8. **Kaido Tammeveski.** Oxygen electroreduction on thin platinum films and the electrochemical detection of superoxide anion. Tartu, 1998, 139 p.
9. **Ivo Leito.** Studies of Brønsted acid-base equilibria in water and non-aqueous media. Tartu, 1998, 101 p.
10. **Jaan Leis.** Conformational dynamics and equilibria in amides. Tartu, 1998, 131 p.
11. **Toonika Rinken.** The modelling of amperometric biosensors based on oxidoreductases. Tartu, 2000, 108 p.
12. **Dmitri Panov.** Partially solvated Grignard reagents. Tartu, 2000, 64 p.
13. **Kaja Orupõld.** Treatment and analysis of phenolic wastewater with microorganisms. Tartu, 2000, 123 p.
14. **Jüri Ivask.** Ion Chromatographic determination of major anions and cations in polar ice core. Tartu, 2000, 85 p.
15. **Lauri Vares.** Stereoselective Synthesis of Tetrahydrofuran and Tetrahydropyran Derivatives by Use of Asymmetric Horner-Wadsworth-Emmons and Ring Closure Reactions. Tartu, 2000, 184 p.
16. **Martin Lepiku.** Kinetic aspects of dopamine D_2 receptor interactions with specific ligands. Tartu, 2000, 81 p.
17. **Katrin Sak.** Some aspects of ligand specificity of P2Y receptors. Tartu, 2000, 106 p.
18. **Vello Pällin.** The role of solvation in the formation of iotsitch complexes. Tartu, 2001, 95 p.
19. **Katrin Kollist.** Interactions between polycyclic aromatic compounds and humic substances. Tartu, 2001, 93 p.

20. **Ivar Koppel.** Quantum chemical study of acidity of strong and superstrong Brønsted acids. Tartu, 2001, 104 p.
21. **Viljar Pihl.** The study of the substituent and solvent effects on the acidity of OH and CH acids. Tartu, 2001, 132 p.
22. **Natalia Palm.** Specification of the minimum, sufficient and significant set of descriptors for general description of solvent effects. Tartu, 2001, 134 p.
23. **Sulev Sild.** QSPR/QSAR approaches for complex molecular systems. Tartu, 2001, 134 p.
24. **Ruslan Petrukhin.** Industrial applications of the quantitative structure-property relationships. Tartu, 2001, 162 p.
25. **Boris V. Rogovoy.** Synthesis of (benzotriazolyl)carboximidamides and their application in relations with *N*- and *S*-nucleophyles. Tartu, 2002, 84 p.
26. **Koit Herodes.** Solvent effects on UV-vis absorption spectra of some solvatochromic substances in binary solvent mixtures: the preferential solvation model. Tartu, 2002, 102 p.
27. **Anti Perkson.** Synthesis and characterisation of nanostructured carbon. Tartu, 2002, 152 p.
28. **Ivari Kaljurand.** Self-consistent acidity scales of neutral and cationic Brønsted acids in acetonitrile and tetrahydrofuran. Tartu, 2003, 108 p.
29. **Karmen Lust.** Adsorption of anions on bismuth single crystal electrodes. Tartu, 2003, 128 p.
30. **Mare Piirsalu.** Substituent, temperature and solvent effects on the alkaline hydrolysis of substituted phenyl and alkyl esters of benzoic acid. Tartu, 2003, 156 p.
31. **Meeri Sassian.** Reactions of partially solvated Grignard reagents. Tartu, 2003, 78 p.
32. **Tarmo Tamm.** Quantum chemical modelling of polypyrrole. Tartu, 2003. 100 p.
33. **Erik Teinemaa.** The environmental fate of the particulate matter and organic pollutants from an oil shale power plant. Tartu, 2003. 102 p.
34. **Jaana Tammiku-Taul.** Quantum chemical study of the properties of Grignard reagents. Tartu, 2003. 120 p.
35. **Andre Lomaka.** Biomedical applications of predictive computational chemistry. Tartu, 2003. 132 p.
36. **Kostyantyn Kirichenko.** Benzotriazole – Mediated Carbon–Carbon Bond Formation. Tartu, 2003. 132 p.
37. **Gunnar Nurk.** Adsorption kinetics of some organic compounds on bismuth single crystal electrodes. Tartu, 2003, 170 p.
38. **Mati Arulepp.** Electrochemical characteristics of porous carbon materials and electrical double layer capacitors. Tartu, 2003, 196 p.
39. **Dan Cornel Fara.** QSPR modeling of complexation and distribution of organic compounds. Tartu, 2004, 126 p.
40. **Riina Mahlapuu.** Signalling of galanin and amyloid precursor protein through adenylate cyclase. Tartu, 2004, 124 p.

41. **Mihkel Kerikmäe.** Some luminescent materials for dosimetric applications and physical research. Tartu, 2004, 143 p.
42. **Jaanus Kruusma.** Determination of some important trace metal ions in human blood. Tartu, 2004, 115 p.
43. **Urmas Johanson.** Investigations of the electrochemical properties of polypyrrole modified electrodes. Tartu, 2004, 91 p.
44. **Kaido Sillar.** Computational study of the acid sites in zeolite ZSM-5. Tartu, 2004, 80 p.
45. **Aldo Oras.** Kinetic aspects of dATPαS interaction with $P2Y_1$ receptor. Tartu, 2004, 75 p.
46. **Erik Mölder.** Measurement of the oxygen mass transfer through the air-water interface. Tartu, 2005, 73 p.
47. **Thomas Thomberg.** The kinetics of electroreduction of peroxodisulfate anion on cadmium (0001) single crystal electrode. Tartu, 2005, 95 p.
48. **Olavi Loog.** Aspects of condensations of carbonyl compounds and their imine analogues. Tartu, 2005, 83 p.
49. **Siim Salmar.** Effect of ultrasound on ester hydrolysis in aqueous ethanol. Tartu, 2006, 73 p.
50. **Ain Uustare.** Modulation of signal transduction of heptahelical receptors by other receptors and G proteins. Tartu, 2006, 121 p.
51. **Sergei Yurchenko.** Determination of some carcinogenic contaminants in food. Tartu, 2006, 143 p.
52. **Kaido Tämm.** QSPR modeling of some properties of organic compounds. Tartu, 2006, 67 p.
53. **Olga Tšubrik.** New methods in the synthesis of multisubstituted hydrazines. Tartu. 2006, 183 p.
54. **Lilli Sooväli.** Spectrophotometric measurements and their uncertainty in chemical analysis and dissociation constant measurements. Tartu, 2006, 125 p.
55. **Eve Koort.** Uncertainty estimation of potentiometrically measured ph and pK_a values. Tartu, 2006, 139 p.
56. **Sergei Kopanchuk.** Regulation of ligand binding to melanocortin receptor subtypes. Tartu, 2006, 119 p.
57. **Silvar Kallip.** Surface structure of some bismuth and antimony single crystal electrodes. Tartu, 2006, 107 p.
58. **Kristjan Saal.** Surface silanization and its application in biomolecule coupling. Tartu, 2006, 77 p.
59. **Tanel Tätte.** High viscosity $Sn(OBu)_4$ oligomeric concentrates and their applications in technology. Tartu, 2006, 91 p.
60. **Dimitar Atanasov Dobchev**. Robust QSAR methods for the prediction of properties from molecular structure. Tartu, 2006, 118 p.
61. **Hannes Hagu**. Impact of ultrasound on hydrophobic interactions in solutions. Tartu, 2007, 81 p.
62. **Rutha Jäger.** Electroreduction of peroxodisulfate anion on bismuth electrodes. Tartu, 2007, 142 p.

63. **Kaido Viht.** Immobilizable bisubstrate-analogue inhibitors of basophilic protein kinases: development and application in biosensors. Tartu, 2007, 88 p.
64. **Eva-Ingrid Rõõm.** Acid-base equilibria in nonpolar media. Tartu, 2007, 156 p.
65. **Sven Tamp.** DFT study of the cesium cation containing complexes relevant to the cesium cation binding by the humic acids. Tartu, 2007, 102 p.
66. **Jaak Nerut.** Electroreduction of hexacyanoferrate(III) anion on Cadmium (0001) single crystal electrode. Tartu, 2007, 180 p.
67. **Lauri Jalukse.** Measurement uncertainty estimation in amperometric dissolved oxygen concentration measurement. Tartu, 2007, 112 p.
68. **Aime Lust.** Charge state of dopants and ordered clusters formation in CaF_2:Mn and CaF_2:Eu luminophors. Tartu, 2007, 100 p.
69. **Iiris Kahn**. Quantitative Structure-Activity Relationships of environmentally relevant properties. Tartu, 2007, 98 p.
70. **Mari Reinik.** Nitrates, nitrites, N-nitrosamines and polycyclic aromatic hydrocarbons in food: analytical methods, occurrence and dietary intake. Tartu, 2007, 172 p.
71. **Heili Kasuk.** Thermodynamic parameters and adsorption kinetics of organic compounds forming the compact adsorption layer at Bi single crystal electrodes. Tartu, 2007, 212 p.
72. **Erki Enkvist.** Synthesis of adenosine-peptide conjugates for biological applications. Tartu, 2007, 114 p.
73. **Svetoslav Hristov Slavov**. Biomedical applications of the QSAR approach. Tartu, 2007, 146 p.
74. **Eneli Härk.** Electroreduction of complex cations on electrochemically polished Bi(*hkl*) single crystal electrodes. Tartu, 2008, 158 p.
75. **Priit Möller.** Electrochemical characteristics of some cathodes for medium temperature solid oxide fuel cells, synthesized by solid state reaction technique. Tartu, 2008, 90 p.
76. **Signe Viggor.** Impact of biochemical parameters of genetically different pseudomonads at the degradation of phenolic compounds. Tartu, 2008, 122 p.
77. **Ave Sarapuu.** Electrochemical reduction of oxygen on quinone-modified carbon electrodes and on thin films of platinum and gold. Tartu, 2008, 134 p.
78. **Agnes Kütt.** Studies of acid-base equilibria in non-aqueous media. Tartu, 2008, 198 p.
79. **Rouvim Kadis.** Evaluation of measurement uncertainty in analytical chemistry: related concepts and some points of misinterpretation. Tartu, 2008, 118 p.
80. **Valter Reedo.** Elaboration of IVB group metal oxide structures and their possible applications. Tartu, 2008, 98 p.
81. **Aleksei Kuznetsov.** Allosteric effects in reactions catalyzed by the cAMP-dependent protein kinase catalytic subunit. Tartu, 2009, 133 p.

82. **Aleksei Bredihhin.** Use of mono- and polyanions in the synthesis of multisubstituted hydrazine derivatives. Tartu, 2009, 105 p.
83. **Anu Ploom.** Quantitative structure-reactivity analysis in organosilicon chemistry. Tartu, 2009, 99 p.
84. **Argo Vonk.** Determination of adenosine A_{2A}- and dopamine D_1 receptor-specific modulation of adenylate cyclase activity in rat striatum. Tartu, 2009, 129 p.
85. **Indrek Kivi.** Synthesis and electrochemical characterization of porous cathode materials for intermediate temperature solid oxide fuel cells. Tartu, 2009, 177 p.
86. **Jaanus Eskusson.** Synthesis and characterisation of diamond-like carbon thin films prepared by pulsed laser deposition method. Tartu, 2009, 117 p.
87. **Marko Lätt.** Carbide derived microporous carbon and electrical double layer capacitors. Tartu, 2009, 107 p.
88. **Vladimir Stepanov.** Slow conformational changes in dopamine transporter interaction with its ligands. Tartu, 2009, 103 p.
89. **Aleksander Trummal.** Computational Study of Structural and Solvent Effects on Acidities of Some Brønsted Acids. Tartu, 2009, 103 p.
90. **Eerold Vellemäe.** Applications of mischmetal in organic synthesis. Tartu, 2009, 93 p.
91. **Sven Parkel.** Ligand binding to 5-HT_{1A} receptors and its regulation by Mg^{2+} and Mn^{2+}. Tartu, 2010, 99 p.
92. **Signe Vahur.** Expanding the possibilities of ATR-FT-IR spectroscopy in determination of inorganic pigments. Tartu, 2010, 184 p.
93. **Tavo Romann**. Preparation and surface modification of bismuth thin film, porous, and microelectrodes. Tartu, 2010, 155 p.
94. **Nadežda Aleksejeva.** Electrocatalytic reduction of oxygen on carbon nanotube-based nanocomposite materials. Tartu, 2010, 147 p.
95. **Marko Kullapere.** Electrochemical properties of glassy carbon, nickel and gold electrodes modified with aryl groups. Tartu, 2010, 233 p.
96. **Liis Siinor.** Adsorption kinetics of ions at Bi single crystal planes from aqueous electrolyte solutions and room-temperature ionic liquids. Tartu, 2010, 101 p.
97. **Angela Vaasa.** Development of fluorescence-based kinetic and binding assays for characterization of protein kinases and their inhibitors. Tartu 2010, 101 p.
98. **Indrek Tulp.** Multivariate analysis of chemical and biological properties. Tartu 2010, 105 p.
99. **Aare Selberg.** Evaluation of environmental quality in Northern Estonia by the analysis of leachate. Tartu 2010, 117 p.
100. **Darja Lavõgina.** Development of protein kinase inhibitors based on adenosine analogue-oligoarginine conjugates. Tartu 2010, 248 p.
101. **Laura Herm.** Biochemistry of dopamine D_2 receptors and its association with motivated behaviour. Tartu 2010, 156 p.

102. **Terje Raudsepp.** Influence of dopant anions on the electrochemical properties of polypyrrole films. Tartu 2010, 112 p.
103. **Margus Marandi.** Electroformation of Polypyrrole Films: *In-situ* AFM and STM Study. Tartu 2011, 116 p.
104. **Kairi Kivirand.** Diamine oxidase-based biosensors: construction and working principles. Tartu, 2011, 140 p.
105. **Anneli Kruve.** Matrix effects in liquid-chromatography electrospray mass-spectrometry. Tartu, 2011, 156 p.
106. **Gary Urb.** Assessment of environmental impact of oil shale fly ash from PF and CFB combustion. Tartu, 2011, 108 p.
107. **Nikita Oskolkov.** A novel strategy for peptide-mediated cellular delivery and induction of endosomal escape. Tartu, 2011, 106 p.
108. **Dana Martin.** The QSPR/QSAR approach for the prediction of properties of fullerene derivatives. Tartu, 2011, 98 p.
109. **Säde Viirlaid.** Novel glutathione analogues and their antioxidant activity. Tartu, 2011, 106 p.
110. **Ülis Sõukand.** Simultaneous adsorption of Cd^{2+}, Ni^{2+}, and Pb^{2+} on peat. Tartu, 2011, 124 p.
111. **Lauri Lipping.** The acidity of strong and superstrong Brønsted acids, an outreach for the "limits of growth": a quantum chemical study. Tartu, 2011, 124 p.
112. **Heisi Kurig.** Electrical double-layer capacitors based on ionic liquids as electrolytes. Tartu, 2011, 146 p.
113. **Marje Kasari.** Bisubstrate luminescent probes, optical sensors and affinity adsorbents for measurement of active protein kinases in biological samples. Tartu, 2012, 126 p.
114. **Kalev Takkis.** Virtual screening of chemical databases for bioactive molecules. Tartu, 2012, 122 p.
115. **Ksenija Kisseljova**. Synthesis of aza-β^3-amino acid containing peptides and kinetic study of their phosphorylation by protein kinase A. Tartu, 2012, 104 p.
116. **Riin Rebane.** Advanced method development strategy for derivatization LC/ESI/MS. Tartu, 2012, 184 p.
117. **Vladislav Ivaništšev.** Double layer structure and adsorption kinetics of ions at metal electrodes in room temperature ionic liquids. Tartu, 2012, 128 p.
118. **Irja Helm.** High accuracy gravimetric Winkler method for determination of dissolved oxygen. Tartu, 2012, 139 p.
119. **Karin Kipper.** Fluoroalcohols as Components of LC-ESI-MS Eluents: Usage and Applications. Tartu, 2012, 164 p.
120. **Arno Ratas.** Energy storage and transfer in dosimetric luminescent materials. Tartu, 2012, 163 p.
121. **Reet Reinart-Okugbeni**. Assay systems for characterisation of subtype-selective binding and functional activity of ligands on dopamine receptors. Tartu, 2012, 159 p.

122. **Lauri Sikk.** Computational study of the Sonogashira cross-coupling reaction. Tartu, 2012, 81 p.
123. **Karita Raudkivi.** Neurochemical studies on inter-individual differences in affect-related behaviour of the laboratory rat. Tartu, 2012, 161 p.
124. **Indrek Saar.** Design of GalR2 subtype specific ligands: their role in depression-like behavior and feeding regulation. Tartu, 2013, 126 p.
125. **Ann Laheäär.** Electrochemical characterization of alkali metal salt based non-aqueous electrolytes for supercapacitors. Tartu, 2013, 127 p.
126. **Kerli Tõnurist.** Influence of electrospun separator materials properties on electrochemical performance of electrical double-layer capacitors. Tartu, 2013, 147 p.
127. **Kaija Põhako-Esko.** Novel organic and inorganic ionogels: preparation and characterization. Tartu, 2013, 124 p.
128. **Ivar Kruusenberg.** Electroreduction of oxygen on carbon nanomaterial-based catalysts. Tartu, 2013, 191 p.
129. **Sander Piiskop.** Kinetic effects of ultrasound in aqueous acetonitrile solutions. Tartu, 2013, 95 p.
130. **Ilona Faustova**. Regulatory role of L-type pyruvate kinase N-terminal domain. Tartu, 2013, 109 p.
131. **Kadi Tamm.** Synthesis and characterization of the micro-mesoporous anode materials and testing of the medium temperature solid oxide fuel cell single cells. Tartu, 2013, 138 p.
132. **Iva Bozhidarova Stoyanova-Slavova.** Validation of QSAR/QSPR for regulatory purposes. Tartu, 2013, 109 p.
133. **Vitali Grozovski**. Adsorption of organic molecules at single crystal electrodes studied by *in situ* STM method. Tartu, 2014, 146 p.
134. **Santa Veikšina**. Development of assay systems for characterisation of ligand binding properties to melanocortin 4 receptors. Tartu, 2014, 151 p.
135. **Jüri Liiv.** PVDF (polyvinylidene difluoride) as material for active element of twisting-ball displays. Tartu, 2014, 111 p.
136. **Kersti Vaarmets.** Electrochemical and physical characterization of pristine and activated molybdenum carbide-derived carbon electrodes for the oxygen electroreduction reaction. Tartu, 2014, 131 p.
137. **Lauri Tõntson**. Regulation of G-protein subtypes by receptors, guanine nucleotides and Mn^{2+}. Tartu, 2014, 105 p.
138. **Aiko Adamson.** Properties of amine-boranes and phosphorus analogues in the gas phase. Tartu, 2014, 78 p.
139. **Elo Kibena**. Electrochemical grafting of glassy carbon, gold, highly oriented pyrolytic graphite and chemical vapour deposition-grown graphene electrodes by diazonium reduction method. Tartu, 2014, 184 p.
140. **Teemu Näykki.** Novel Tools for Water Quality Monitoring – From Field to Laboratory. Tartu, 2014, 202 p.
141. **Karl Kaupmees.** Acidity and basicity in non-aqueous media: importance of solvent properties and purity. Tartu, 2014, 128 p.

142. **Oleg Lebedev**. Hydrazine polyanions: different strategies in the synthesis of heterocycles. Tartu, 2015, 118 p.
143. **Geven Piir.** Environmental risk assessment of chemicals using QSAR methods. Tartu, 2015, 123 p.
144. **Olga Mazina.** Development and application of the biosensor assay for measurements of cyclic adenosine monophosphate in studies of G protein-coupled receptor signalinga. Tartu, 2015, 116 p.
145. **Sandip Ashokrao Kadam.** Anion receptors: synthesis and accurate binding measurements. Tartu, 2015, 116 p.
146. **Indrek Tallo.** Synthesis and characterization of new micro-mesoporous carbide derived carbon materials for high energy and power density electrical double layer capacitors. Tartu, 2015, 148 p.
147. **Heiki Erikson.** Electrochemical reduction of oxygen on nanostructured palladium and gold catalysts. Tartu, 2015, 204 p.
148. **Erik Anderson.** *In situ* Scanning Tunnelling Microscopy studies of the interfacial structure between Bi(111) electrode and a room temperature ionic liquid. Tartu, 2015, 118 p.
149. **Girinath G. Pillai.** Computational Modelling of Diverse Chemical, Bio-chemical and Biomedical Properties. Tartu, 2015, 140 p.
150. **Piret Pikma.** Interfacial structure and adsorption of organic compounds at Cd(0001) and Sb(111) electrodes from ionic liquid and aqueous electrolytes: an *in situ* STM study. Tartu, 2015, 126 p.
151. **Ganesh babu Manoharan.** Combining chemical and genetic approaches for photoluminescence assays of protein kinases. Tartu, 2016, 126 p.
152. **Carolin Siimenson**. Electrochemical characterization of halide ion adsorption from liquid mixtures at Bi(111) and pyrolytic graphite electrode surface. Tartu, 2016, 110 p.
153. **Asko Laaniste.** Comparison and optimisation of novel mass spectrometry ionisation sources. Tartu, 2016, 156 p.
154. **Hanno Evard.** Estimating limit of detection for mass spectrometric analysis methods. Tartu, 2016, 224 p.
155. **Kadri Ligi.** Characterization and application of protein kinase-responsive organic probes with triplet-singlet energy transfer. Tartu, 2016, 122 p.
156. **Margarita Kagan.** Biosensing penicillins' residues in milk flows. Tartu, 2016, 130 p.
157. **Marie Kriisa.** Development of protein kinase-responsive photo-luminescent probes and cellular regulators of protein phosphorylation. Tartu, 2016, 106 p.
158. **Mihkel Vestli.** Ultrasonic spray pyrolysis deposited electrolyte layers for intermediate temperature solid oxide fuel cells. Tartu, 2016, 156 p.
159. **Silver Sepp**. Influence of porosity of the carbide-derived carbon on the properties of the composite electrocatalysts and characteristics of polymer electrolyte fuel cells. Tartu, 2016, 137p.
160. **Kristjan Haav**. Quantitative relative equilibrium constant measurements in supramolecular chemistry. Tartu, 2017, 158 p.

161. **Anu Teearu**. Development of MALDI-FT-ICR-MS methodology for the analysis of resinous materials. Tartu, 2017, 205 p.
162. **Taavi Ivan**. Bifunctional inhibitors and photoluminescent probes for studies on protein complexes. Tartu, 2017, 140 p.
163. **Maarja-Liisa Oldekop**. Characterization of amino acid derivatization reagents for LC-MS analysis. Tartu, 2017, 147 p.
164. **Kristel Jukk**. Electrochemical reduction of oxygen on platinum- and palladium-based nanocatalysts. Tartu, 2017, 250 p.
165. **Siim Kukk**. Kinetic aspects of interaction between dopamine transporter and *N*-substituted nortropane derivatives. Tartu, 2017, 107 p.
166. **Birgit Viira**. Design and modelling in early drug development in targeting HIV-1 reverse transcriptase and Malaria. Tartu, 2017, 172 p.